

MECHANICAL PROPERTIES OF ICE

Thesis for the Degree of M. S.  
MICHIGAN STATE UNIVERSITY  
Thomas R. Halbrook  
1962

This is to certify that the

thesis entitled

Mechanical Properties Of Ice

presented by

Thomas R. Halbrook

has been accepted towards fulfillment  
of the requirements for

M. S. degree in C. E.

O. B. Andersland

Major professor

Date August 9, 1962





~~H 068~~

~~A 296~~

F 060

~~J 116~~  
~~10 13 178 214~~

~~JAN 7 1993~~  
NOV 22 1993  
~~678638-1~~ 421

**MECHANICAL PROPERTIES OF ICE**

By

**Thomas R. Halbrook**

**AN ABSTRACT**

Submitted to the College of Engineering  
Michigan State University  
in partial fulfillment of the requirements  
for the degree of

**MASTER OF SCIENCE**

**Department of Civil Engineering**

**1962**

## ABSTRACT

### MECHANICAL PROPERTIES OF ICE

by Thomas R. Halbrook

This thesis is an investigation of the mechanical properties of polycrystalline ice in compression and in creep.

The investigation consists of the determination of the compressive strength, modulus of elasticity, an analysis of the minimum and tertiary creep rates, and a study of the deformation characters of the material.

Confined and unconfined triaxial tests were used to determine both stress-strain relationships and creep curves for identical polycrystalline ice specimens at  $-4^{\circ}$  C. The effect of rate of axial deformation was varied in constant-rate-of-strain experiments and creep under constant load were conducted under several large loads.

It was found that by increasing the rate of axial deformation, polycrystalline ice will exhibit larger values for Young's modulus and a larger ultimate strength.

The creep of ice under large loads is greatly influenced by stress level and confinement. Bulk flow laws and simple viscoelastic models will give only rough approximations of behavior. Confining pressure appears to increase

Thomas R. Halbrook

the minimum creep rate and to decrease the tertiary creep rate. Based on strain measurements and the observed influence of confining pressure, it is likely that tertiary creep occurs after the ultimate strain of the material has been exceeded.

**MECHANICAL PROPERTIES OF ICE**

**By**

**Thomas R. Halbrook**

**A THESIS**

**Submitted to the College of Engineering  
Michigan State University  
in partial fulfillment of the requirements  
for the degree of**

**MASTER OF SCIENCE**

**Department of Civil Engineering**

**1962**

## ACKNOWLEDGEMENTS

The author wishes to express his deep gratitude for the guidance and inspiration of Dr. O. B. Andersland, Assistant Professor of Civil Engineering, Michigan State University, under whose supervision this study was conducted.

Special thanks are due Mr. John W. Hoffman, Director of Engineering Research, Michigan State University, for the equipment made available through his office; and to Dr. George Mase, Professor of Applied Mechanics, Michigan State University, for his valuable advice concerning the visco-elastic properties of engineering materials.

The author is indebted to his colleagues, B. N. Beyleryan, A. K. Loh, and R. W. Christensen, for their thoughtful suggestions and help in the testing and analysis. Through the efforts of Mr. Leo Szafranski, our departmental mechanic, costly time delays were avoided; the author is grateful for his help.

Finally, the writer would like to thank his wife for typing the draft and final copy of the thesis. Without her warm encouragement and understanding this thesis would not have been possible.

## TABLE OF CONTENTS

	Page
<b>ACKNOWLEDGEMENTS</b> . . . . .	11
<b>LIST OF TABLES</b> . . . . .	v
<b>LIST OF FIGURES</b> . . . . .	vi
 <b>Chapter</b>	
<b>I. INTRODUCTION</b> . . . . .	1
<b>II. MECHANICAL PROPERTIES OF ICE, LITERATURE REVIEW</b> . . . . .	6
Compressive Strength . . . . .	9
Tensile Strength . . . . .	14
Shearing Strength . . . . .	17
Elastic Properties . . . . .	18
Creep . . . . .	22
Primary Creep . . . . .	24
Secondary Creep . . . . .	25
Tertiary Creep . . . . .	32
Activation Energy . . . . .	33
Effect of Confining Pressure on Creep . . . . .	38
Viscoelastic Properties . . . . .	40
<b>III. APPARATUS AND PROCEDURES</b> . . . . .	51
<b>IV. EXPERIMENTAL RESULTS AND DISCUSSION</b> . . . . .	65
Results of Constant Rate of Axial Deformation Experiments . . . . .	65
Results of Creep Experiments . . . . .	80
Minimum Creep Rate Observations . . . . .	84
Tertiary Creep Observations . . . . .	90
<b>V. CONCLUSIONS</b> . . . . .	99

	<b>Page</b>
<b>RECOMMENDATIONS FOR FUTURE WORK . . . . .</b>	<b>101</b>
<b>BIBLIOGRAPHY . . . . .</b>	<b>102</b>
<b>APPENDICES . . . . .</b>	<b>105</b>
<b>A Detailed Procedures . . . . .</b>	<b>106</b>
<b>B Data . . . . .</b>	<b>108</b>

LIST OF TABLES

Table	Page
1. Summary of Previous Investigations of Secondary Creep . . . . .	31
2. Activation Energy of Ice . . . . .	36
3. Summary of Constant-Rate-of-Strain Results . . .	73
4. Summary of Creep Results . . . . .	86
5. Seating Strain Observations . . . . .	109

## LIST OF FIGURES

Figure	Page
1. Structure of a Frozen Soil . . . . .	3
2. Stress on an Ice Crystal in Frozen Soil . . . . .	3
3. Molecular Structure of Ice . . . . .	7
4. Unconfined Compressive Strength of Ice Versus Temperature . . . . .	12
5. Average Tensile Strength As a Function of Load Application . . . . .	15
6. Typical Creep Curve . . . . .	23
7. Variation of Minimum Creep Rate With Compressive Stress . . . . .	28
8. Variation of Creep With Shear Stress . . . . .	34
9. Variation of the Activation Energy of Ice With Stress . . . . .	39
10. Influence of Confining Pressure on Creep . . . . .	41
11. Basic Viscoelastic Models . . . . .	43
12. Behavior of a Burgers Model in Creep and Relaxation . . . . .	46
13. Disassembled Aluminum Ice Mold, Specimens, and Loading Paraphernalia . . . . .	52
14. Schematic Diagram of Ice Specimen Prepared for Testing . . . . .	55
15. Test Equipment . . . . .	58
16. Schematic Diagram of Hydraulic and Cooling System . . . . .	60
17. Temperature Measuring Equipment . . . . .	63

Figure	Page
18. Typical Appearance of Specimens After Testing	66
19. Typical Response of Ice Subjected to a Constant Rate of Axial Deformation . . . . .	68
20. a, b, c, d, Stress-Strain Curves for Ice . . . .	69
21. Variation of Young's Modulus of Ice With Strain Rate . . . . .	75
22. Variation of Ultimate Strength of Ice With Strain Rate . . . . .	77
23. Mohrs Circle for Polycrystalline Ice . . . . .	79
24. a, b, c, Creep Curves of Ice Under Constant Load . . . . .	81
25. Variation of Minimum Creep With Load, Time and Confinement . . . . .	87
26. Variation of a Function of Tertiary Creep Strain With Time and Confining Pressure . . . . .	91
27. Variation of the Exponent of Time for Tertiary Creep With Load and Confinement . . . . .	93
28. Comparison of a Typical Stress-Strain Curve to a Typical Creep Curve . . . . .	95

## CHAPTER I

### INTRODUCTION

During the last ten years a great deal of attention has been given to the mechanical properties of ice. Since the early 1950's, the United States Army Corps of Engineers have added much knowledge to the field of ice mechanics through their studies pertaining to tunnels and cavities built in the Greenland Ice Cap. Many other organizations are interested in the behavior of ice as it relates to the properties of frozen soils. Prior to this time much of the investigation was conducted by geologists searching for answers to the riddle of glacial movement.

The work done to date concerns itself primarily with the behavior of ice under low stress. Knowledge of ice mechanics under high stress is practically nonexistent, and very little is known about the effect of confining pressure. It is reasonable to expect that ice contained in soil pores will be subjected to high stresses, values approximating pressures between point contacts of individual soil particles.

All the water in a frozen soil mass is not frozen. Substantial proportions do not freeze at temperatures as low as  $-20^{\circ}$  C. (Lovell, 1957). The amount of freezing that occurs depends upon the temperature, soil type and arrangement of the soil particles (Jackson and Chalmers, 1957; Chalmers, 1960)

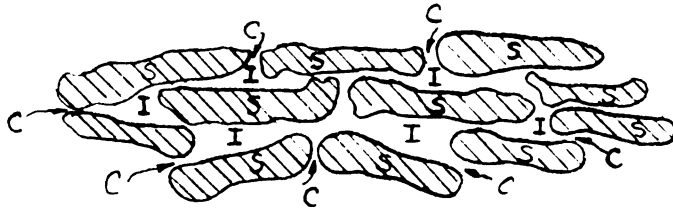
and the ions in the absorbed water layer surrounding the soil particles (Leonards and Andersland, 1960).

Figure 1a shows a typical structure of a claylike soil. The channels and interstices (voids) of the mass may be filled with water and/or air, while the amount of water is referred to as the moisture content. Nucleation can only occur when the radius of curvature of the water within the interstices and channels has a magnitude greater than the critical radius for the prevailing temperature (Jackson and Chalmers, 1958). Ice will form in the larger interstices before it forms in the channels as shown in Figure 1b. At a given temperature the ice structure within a soil mass is composed of many individual crystals of ice that are polycrystalline in nature (Chalmers, 1960). It is reasonable that the properties of polycrystalline ice contained in the soil pores play a major role in the shear strength of frozen soil.

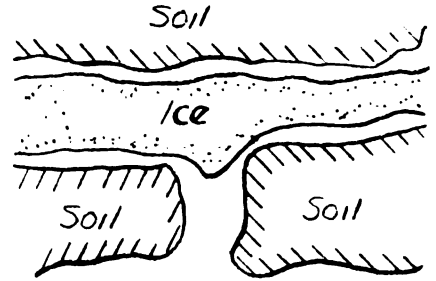
It can be shown that the ice within the interstices is subjected to large pressures using the analysis given by Skempton (1961). With reference to Figure 2, consider a particle of ice in contact with a particle of soil on some statistical plane,  $A_s$ , and occupying a gross area,  $A$ , in a plane parallel to this contact. Skempton (1961) defines the contact area ratio,  $a$ , as follows:

$$a = \frac{A_s}{A} \quad ; \quad \therefore a < 1$$

If the force normal to the contact plane is  $P$  and the shear



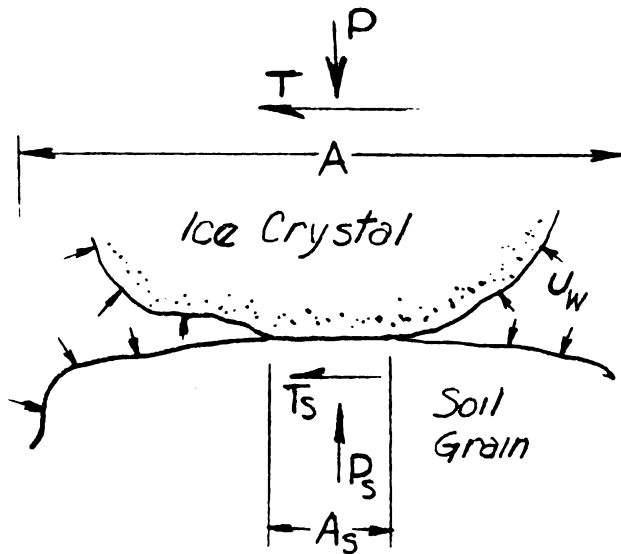
Structure of Soil (Chalmers, 1960)  
 S, Soil Particles; I, Interstices; C, Channels  
 Figure 1a



Formation of Ice in the Interstices  
 Figure 1b

Structure of a Frozen Soil

Figure 1



Stress on an Ice Crystal in Frozen Soil

Figure 2

force is  $T$ , the total normal stress,  $\sigma$ , and the shear stress,  $\tau$ , are

$$\sigma = \frac{P}{A} \quad \text{and} \quad \tau = \frac{T}{A} .$$

Stresses at the interfacial contact are

$$\sigma_s = \frac{P_s}{A_s} \quad \text{and} \quad \tau_s = \frac{T_s}{A_s} .$$

If  $a \simeq 0.1$ , then  $\sigma_s$  would be ten times  $\sigma$ , a fairly large stress. The unfrozen pore water contributes an additional amount of pressure,  $u$ . In kaolinite clays this unfrozen water at a distance of  $10 \text{ \AA}$  from the soil particle can withstand a normal stress of 25 atmospheres (Martin, 1959).

For equilibrium normal to the plane

$$P = P_s + (A - A_s) u .$$

Hence,

$$\sigma = a \cdot \sigma_s + (1 - a) u \quad \text{and} \quad a = \frac{\sigma - u}{\sigma_s - u} .$$

Since  $a$  is less than one, it follows that the contact stress is somewhat larger than the gross stress acting on the section.

The purpose of this thesis is to provide a platform for more extensive work in the field of frozen soil mechanics, primarily through a review of existing literature on ice and several series of experiments on polycrystalline ice. The

influence of varying constant rates of deformation has been investigated. This has often been used to explain the variability of experimental results. Temperature is made a constant ( $-4^{\circ}$  C). The creep properties of ice have been investigated in the past, however only in relatively low stress ranges. A limited investigation of high stress creep has been conducted. The above two series are subjected to a third variable, confining pressure, in order that its effect may be better understood.

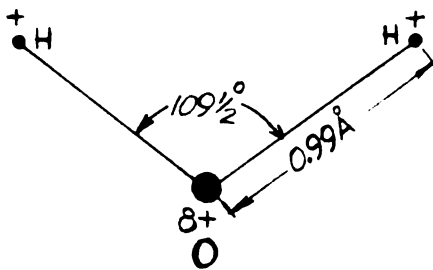
## CHAPTER II

### MECHANICAL PROPERTIES OF ICE--LITERATURE REVIEW

The mechanical properties of ice are related to the molecular structure of an ice crystal. Figure 3a shows the atomic arrangement of a single  $H_2O$  molecule (Bjerrum, 1952). The atoms arrange themselves in "puckered hexagonal layers" (op. cit.) as shown in Figure 3b. The oxygen atoms are shown as black dots and the bonding provided by the hydrogen atoms are the black connecting lines. The number of bonds perpendicular to these layers is small (Figure 3b); and it is along these planes that slippage occurs. These planes are called gliding planes or basal planes.

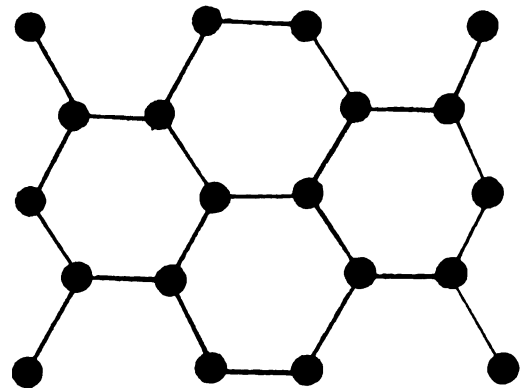
Glen and Perutz (1954) and, independently, Steinemann (1954) reach the conclusion that only along these basal planes does gliding take place during creep. Their conclusion is supported by testing ice crystals with varying tilts of the basal planes and by x-ray diffraction studies of the crystals.

The method of preparing or obtaining ice crystals can be done in several ways. Single crystals of reasonably good quality can be grown using a technique perfected by Landauer (1958). Large single ice crystals have been taken from glaciers, but obtaining and transporting them is difficult and expensive.

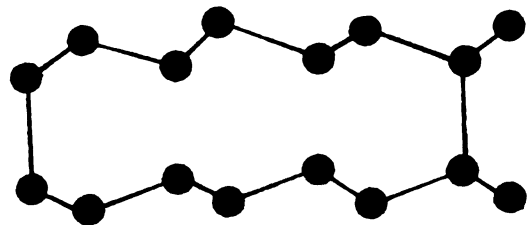


*Electrostatic Model of  
a H<sub>2</sub>O Molecule Showing  
Location of Positively  
Charged Nuclei*

*Figure 3a*



*Top View*



*Side View*

*Molecular Arrangement of  
an Ice Crystal*

*Figure 3b*

*From Bjerrum (1952)*

*Molecular Structure of Ice*

*Figure 3*

Preparing single crystals of ice for testing usually requires forming a specimen into a given shape, (cube, cylinder, hollow cylinder, etc.). Stresses introduced on the surface of the specimen during preparation are thought to be a prime source of the erratic behavior of the results in ice experiments (Jellinek, 1957; Nakaya, 1958; Butkovich, 1954). SIPRE<sup>1</sup> investigators have in the past prepared samples by sawing blocks and beams from larger ice samples, trimming them on a lathe, sandpapering and finishing them to a high gloss with silk, and planing them with a carpenter's plane.

Polycrystalline ice samples, as compared to single crystal samples, are more readily prepared. Duplicating the samples is important, with single crystals this is extremely difficult to accomplish. The properties of an aggregate polycrystalline sample are not always simply statistical averages of the properties of a single crystal taken over all orientations. While this is approximately true of properties which depend primarily on the bulk structure, like the elastic modulus, it is not necessarily true of plastic phenomena (Hill, 1956).

Many investigators have pointed out that air in the water causes voids in the ice samples, altering the physical properties and characteristics. This is overcome by "de-airing" the water by boiling it beforehand.

---

<sup>1</sup>SIPRE refers to the United States Army Corps of Engineers' Snow, Ice and Permafrost Research Establishment at Wilmette, Illinois.

Leonards and Andersland (1960) prepared ice cylinders in an aluminum mold by supercooling distilled, de-aired water. These samples required trimming only on the cylinder top. Their procedure allows many samples to be prepared under identical conditions.

When ice is frozen by supercooling (specially purified water can be cooled to below  $-20^{\circ}$  F before freezing occurs) two distinct processes occur--nucleation and growth. Nucleation is the initiation of freezing that takes place below  $32^{\circ}$  F, and the subsequent freezing that occurs is referred to as growth (Chalmers, 1960). When nucleation occurs, latent heat is given off into the surrounding water, which is then warmer. Further cooling again brings the water below the freezing point and the growth process begins. Ice crystals formed in layers have a dendritic shape and continue to grow on their basal planes as heat is removed through conduction.

Steinemann (1954) discusses physical characteristics of ice formed by supercooling at  $-1^{\circ}$  C and  $-5^{\circ}$  C. In the first case many faults in the linear structure form, but few sub-microscopic faults exist. Ice formed at  $-5^{\circ}$  C always led to the growth of nearly perfect crystals in every direction.

#### Compressive Strength

The compressive strength of ice has been extensively investigated. An excellent summary of the results prior to

1951 may be found in the companion volume of SIPRE Report Number 8 (Volume II, Appendix B, Table 12). The samples ranged in source from poor quality pond ice and various layers of river ice to artificially prepared ice. The majority of the tests were performed on cubes or blocks. Many of the reported investigations did not state the shape of the test sample.

According to the SIPRE table, Vitman and Shandrikov (1938) were the only investigators who studied the strength by means of constant rate of strain (0.1 mm per second).<sup>1</sup> The tests were performed on river ice cubes 1.97 inches on a side. Many preferred to investigate compressive strength from a constant rate of stress increase (psi/minute), however, this information is lacking in numerous cases.

Vitman and Shandrikov's results show a general increase in the strength of ice as the temperature is decreased. However, they report a rather sizeable variation in the strength observed. At  $-4^{\circ}\text{C}$  ( $24.8^{\circ}\text{F}$ ) an interpolation of their results shows that the average strength would be about 180 psi with a maximum of 290 psi and a minimum of 100 psi. Brown (1926) reported a similar increase in strength corresponding to lower temperatures, but his results as to magnitude of strength are not in agreement with those found by Vitman and Shandrikov. This strength variation is believed to take origin in the methods used to prepare and test the

---

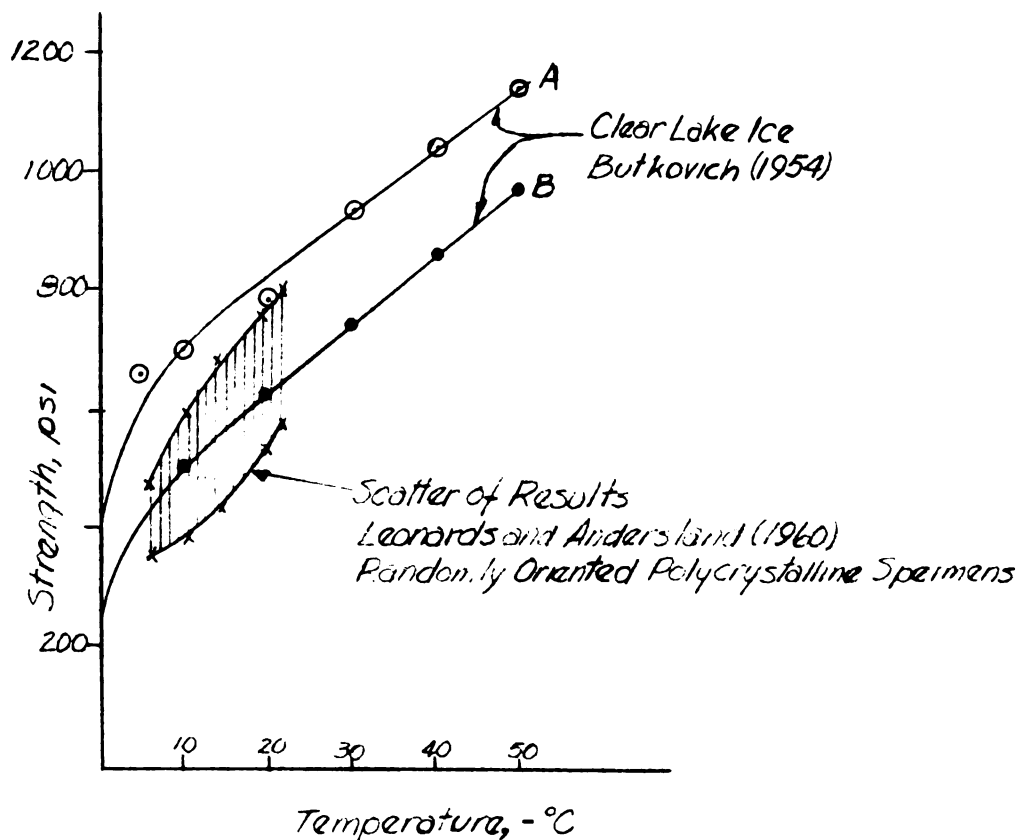
<sup>1</sup>Corresponds to a rate of 12% of the original sample height per minute.

specimens.

In summary, no definite correlation between temperature and compressive strength, in fact, not even a definite average compressive strength can be established from the results of investigations prior to 1951. The Frost Effects Laboratory, which performed the work in SIPRE Report Number 8, found that the following variables have a profound influence upon the compressive strength of ice:

- 1) A sample having a number of small crystals has a greater strength than a sample having one or two crystals.
- 2) The uniformity of loading has an effect upon the failure mode which may occur as one unit or as a group of columns. Columnar failure was not uncommon.
- 3) At constant temperature, a very rough trend toward increased strength with increased rate of loading is indicated.

T. R. Butkovich (1954) performed a series of tests on cylindrical ice specimens to determine the ultimate strength of ice. He used lake ice, natural snow ice, and commercial ice. The specimens had a width-to-height ratio of 1 to 3, which he states is a recommended ratio. His review of literature shows that after extensive testing, during the building of the Southern Manchurian Railway, the Japanese had formulated empirical relationships for crushing strength which



- A. Load Applied Normal to ice sheet (Parallel to Long Axis of Prismatic Crystals).
- B. Load Applied Parallel to Ice Sheet (Normal to Long Axis of Prismatic Crystals).

### Unconfined Compressive Strength of Ice

Figure 4

showed a linear increase of strength with decreasing temperature. However, their results were highly scattered.

His results from ice in compression showed conclusively that temperature had a pronounced effect on ice. A typical curve is that of clear lake ice from Portage, Michigan, shown in Figure 4. An important conclusion is that the strength is indeed dependent upon how the load is applied to the ice sheet itself. Again, a wide variation in strength was observed. His results showed a variation of as much as 140 psi from the mean strength. The mean was obtained from the results of ten samples. All samples were tested in unconfined compression, loading with a rate of approximately  $5 \text{ kg/cm}^2\text{-sec}$ . The specimens were loaded manually and the failure progression was described as follows:

When the load was applied parallel to the length of the prismatic crystals small cracks began to appear inside the ice specimens. They increased in size and number, particularly just before breaking. The time when the cracks first appeared was different for loading normal to the candles, and the cracks first appeared at an angle of  $45^\circ$  near the ends. Chamois skin or sponge rubber was used to seat the ice samples in the crushing apparatus. Temperatures were accurate to  $\pm 1.0^\circ \text{ C}$ .

In 1960 Leonards and Andersland found that the strength of ice increases approximately 15 psi per degree centigrade in their unconfined compression tests using identical, polycrystalline cylindrical samples. Their results showed good agreement with those of Butkovich (see Figure 4).

Interpolating from their curves, ice formed in this manner at  $-4^\circ \text{ C}$  has an average strength of about 370 psi with

a maximum of 430 psi and a minimum of 310 psi. They used a constant rate of strain throughout the series of 2% of the original height per minute.

### Tensile Strength

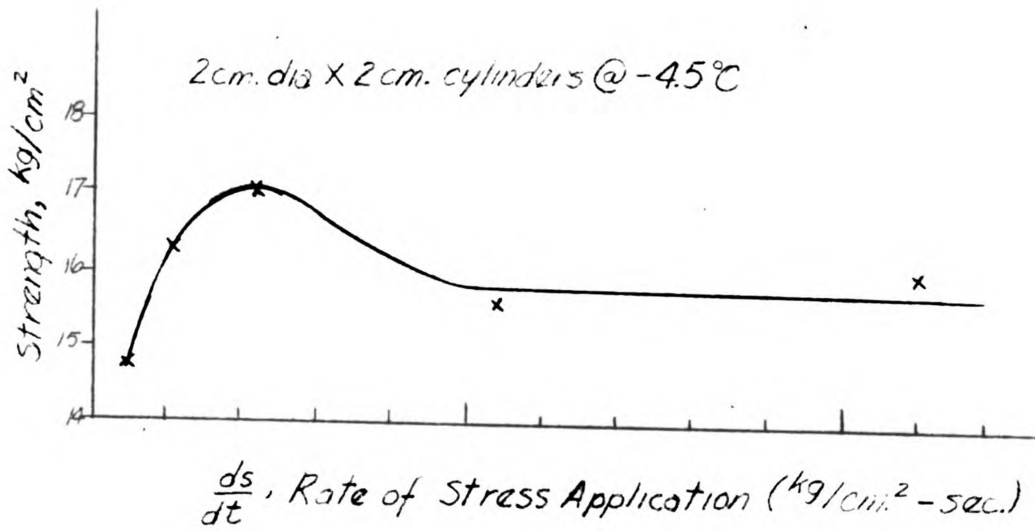
Previous to 1954, very few measurements of the tensile strength of ice were made. The information was computed from observations of other properties, such as the bending of ice beams. Butkovich (1954) pulled cylindrical ice specimens in an electro-hydraulic tensile testing machine. He found a slight increase of tensile strength with decreasing temperature for large grain commercial ice. Because his tests were of sizeable specimens, his results are called bulk tensile strength.

Butkovich's technique for holding the specimen during tension testing was to grip the specimen with a wire. Jellinek and Brill (1956) improved the procedure by freezing the specimens to a roughened metal plate.

In later, more complete, studies of tension by Jellinek (1957), great care was taken to adhere the ice to polished stainless steel. He found definite indications that there were certain stress concentrations at the ice-metal interface, eventually causing failure at this joint.

On large samples he found that the tensile strength was affected by rate of loading (Figure 5). His explanation of this behavior is:

At low speeds of loading, an appreciable plastic flow takes place. Hence, an appreciable lateral stress component



From H. H. G. Jellinek (1957)

Average Tensile Strength as a Function of Load Application Rate

Figure 5

will be present in the neighborhood of the interface, and though counteracted by a certain amount of stress relaxation, (Ed. this stress component) will lead to smaller tensile strength values. At higher speeds of loading, less plastic flow will take place and the lateral stress component will decrease. Therefore, the tensile strength should be higher than at relatively low rates of loading. However, at the high rates the stress relaxation will be small, which in turn will tend to decrease the tensile strength. Hence, there will be an optimum region of loading rates where all these effects will combine to give a maximum tensile strength . . .

However, when Jellinek tested very thin ice discs, different characteristics were observed. A complete cohesive break occurred (the larger samples seemed to partially "peel" off their mountings) and the tensile strength was found to be a function of volume, thickness, and diameter of the disc. However, this apparent correlation between strength and the height-to-diameter relationship, based on the assumption that the tensile strength changes with geometric considerations, was found to be untenable. By a statistical analysis Jellinek concluded that this behavior of the discs is best explained by the imperfections in the ice. He assumed that there is a definite distribution of imperfections, and that these imperfections can stand stresses up to a critical stress, which, if exceeded, causes a crack to open and rupture occurs. In the larger samples the whole distribution of imperfections will be represented from the weakest to the strongest; in the small specimens only those in the neighborhood of the distribution maximum will predominate.

His analysis showed good agreement with the experimental model, and he concludes that tensile strength is

largely governed by the imperfections in the small specimens. In the case of large specimens, the failure near the interface was due to stress concentrations and imperfections. He states that since his statistical method is only an approximation, there is the possibility that a stress distribution effect is present.

### Shearing Strength

The nature of ice in creep alone seems to indicate that shearing forces play a major role in the behavior of ice. To date, however, only one attempt to measure the shearing strength of ice can be located, and the reliability of it is questionable.

The Frost Effects Laboratory (1952) attempted to determine the shearing strength by use of Mohr diagrams. To do so they used tension results and compression results without confining pressure, and their results must be thought of as temporary resistance to shear (units are psi/min). Criticism of their work (Plate 76), in view of more recent findings, would include:

- 1) Rate of stress application for tension specimens was 1/10 of the rate of that for compression specimens. Consistently through the years the effect of varying rates of stress application has been pointed out as having some influence upon the strength of ice.
- 2) The specimens themselves varied both in

crystalline structure and method of forming the samples. Stresses produced in the samples during trimming could have been large.

- 3) Tension failures gave poor results; failures near the gripping surface occurred.
- 4) Results used to produce the average values varied from maximum to minimum as much as 680 psi--a value greater than the average strength itself.
- 5) Two values of  $\phi$ , the angle of internal friction, are obtained, apparently dependent upon the temperature at which the test was conducted. Their calculations of shear strength use  $\phi = 30^\circ$ .

It is interesting to note that comparable results were obtained between the shear strength based on a Mohr's envelope with  $\phi = 30^\circ$ , and the strength obtained from direct shear tests.

#### Elastic Properties

Because ice is not an elastic material, but rather a viscoelastic material, the concept of "elastic" properties of ice are misleading. However, some of the previously determined values are noteworthy.

In 1928, Voigt described the elastic behavior of single ice crystals as being a summation of six elastic moduli and/or six elastic coefficients by the following relationships:

$$\sigma_i = \sum_{n=1}^6 c_{ik} \epsilon_k \quad \text{and} \quad \epsilon_i = \sum_{n=1}^6 s_{ik} \sigma_k$$

$\sigma$  is the stress,  $\epsilon$  the strain,  $C_{ijk}$  the elastic moduli and  $S_{ijk}$  the elastic coefficients. Stephens (1958) reports the results of several investigators who by various sonic methods have determined these elastic constants. As ice is hexagonal, there are five independent elastic constants ( $C_{ijk}$  or  $S_{ijk}$ ). This may be verified by the relationships between the elastic moduli and coefficients.

$$\sum_{n=1}^6 C_{ijk} S_{ijk} = \begin{cases} 1 & \text{for } i = j \\ 0 & \text{for } i \neq j \end{cases}$$

Because ice does have viscoelastic properties, dynamic methods give the only reliable results.

Stephen's summary of the work done shows that temperature does affect the elastic constants, but only in a very small degree. This is to be expected, the values of elastic moduli of crystalline solids will tend to decrease slightly as their melting point is approached (Jastrzebski, 1959). Stephens reports the values of the elastic constants for ice.

The value of Young's modulus determined from these values will vary with the crystal arrangement (strains or stresses in the  $k^{\text{th}}$  direction must be observed or computed respectively). Variations in experimentally determined values of  $E$  are explained by considering that  $E$  depends upon the preferred orientation of the grains (Van Vlack, 1959). The Young's modulus of specimens prepared with random orientation will represent an approximate average value.

The review of the literature completed by the Frost Effects Laboratory for SIPRE (1952) shows that investigations of Young's modulus for ice have given comparable results since 1885. As the temperature decreases, the value of Young's modulus increases slowly. Their linear relationship gives E of  $1.25 \times 10^6$  psi at  $32^\circ$  F and  $1.52 \times 10^6$  psi at  $-34^\circ$  F. The values were obtained from both sonic and static test methods. The static methods were primarily beam flexure tests.

It is important to realize that these values represent the initial tangential modulus, and will be higher than the secant modulus which is conventionally used in engineering design problems.

Nakaya (1959) observed a hysteresis phenomenon in the relationship between Young's modulus and temperature. A similar effect is produced in metals when they are hardened by quenching. The values of E measured as a specimen cooled were found to be lower than the values measured from the same specimen as it was allowed to warm. As the temperature of the warming specimen approached the temperature at which the experiment began, the values of E warming approached the earlier values of E cooling producing the hysteresis curve.

The density of ice has a pronounced effect upon the value of Young's modulus (Nakaya, 1959; Halvorsen, 1959). As the density decreases, a corresponding decrease in the value of Young's modulus occurs. Nakaya's results showed for densities between 0.915 and 0.903 the Young's modulus varied

from  $1.33 \times 10^6$  psi to  $1.09 \times 10^6$  psi respectively. He used a sonic technique and his results agree well with those previously found by other investigators.<sup>1</sup>

The rate of stress application has a pronounced effect upon the elastic properties of ice and is thought to be caused by the viscous nature of ice. The influence of this viscous nature was also noticed in tests on snow ice beams used to determine the elastic modulus (Halvorsen, 1959). Halvorsen found that his values of E varied between 173,500 psi and 194,000 psi ( $1.22 \times 10^4$  kg/cm<sup>2</sup> to  $1.35 \times 10^4$  kg/cm<sup>2</sup>) as the rate of load application varied. The higher values were obtained at faster loading rates.

Poisson's ratio,  $\mu$ , has often been calculated for ice with values ranging from 0.29 to 0.365. Recent investigators (Jellinek, 1959; SIPRE Report 8, 1952; Jellinek and Brill, 1956) have preferred 0.30 as the representative Poisson's ratio for ice. The value of Young's modulus, in conjunction with either Poisson's ratio,  $\mu$ , or the bulk modulus, B, or the shear modulus, G, may be regarded as fundamental and sufficient to calculate the other two properties (Jastrebski, 1959).

---

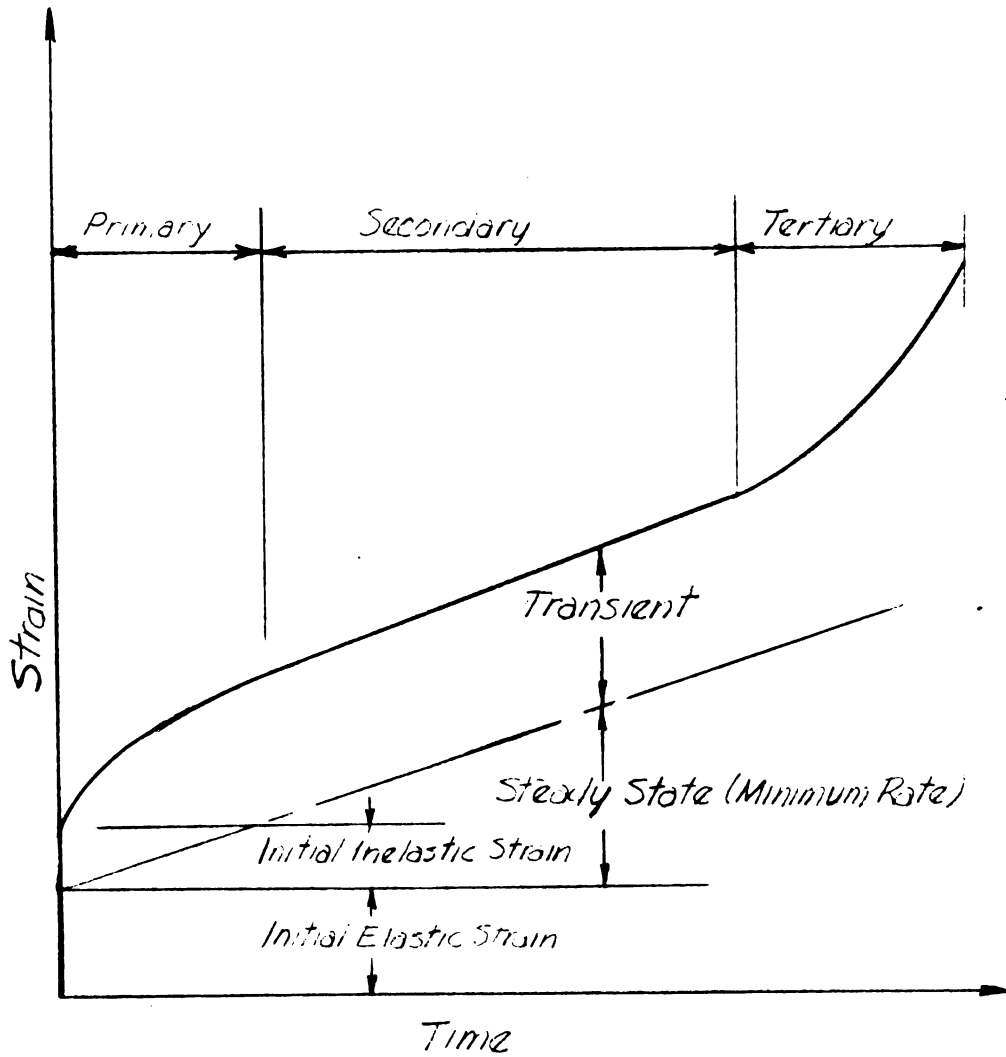
<sup>1</sup>Using resonant frequency to determine Young's modulus has one drawback; the modulus for many viscoelastic materials has been found to be quite sensitive to the frequency at which it is measured. Nakaya (1959) reports that although this frequency dependence is complicated, the effect is not very great for ice. His values for E were corrected for frequency dependence.

### Creep

The relation between stress, strain, and time for ice has been investigated by many authors. Creep has been observed at very low stress levels (Jellinek and Brill, 1956). Because creep is influenced by temperature, the problem of relating creep behavior by bulk flow laws is complex.

Single ice crystals behave somewhat like polycrystalline ice (Butkovich and Landauer, 1959; Jellinek and Brill, 1956). Butovich and Landauer (1959) find that the scatter of results between different types of ice specimens is comparable to the scatter of results between specimens of the same type.

A typical creep curve is shown in Figure 6, in which the three basic stages of creep are illustrated (Finnie and Heller, 1959). Primary creep of ice consists of an initial elastic strain (which can be recovered after unloading) and an initial inelastic strain (which is not recoverable). Following these initial strains is a transient stage in which the creep rate rapidly decreases, eventually slowing down to a minimum, which is called the secondary creep stage. Tertiary creep, the third stage, occurs at a faster rate than the secondary or minimum creep rate. This behavior is thought to be a result of intercrystalline movement as opposed to the intracrystalline movement of primary and secondary creep rates. Tertiary creep can occur at any temperature providing the stress level is high. In metals,



(From: Finnie and Haller, 1959)

Typical Creep Curve

Figure 6

near their melting points, tertiary creep has occurred under low stresses (Finnie and Heller, 1959).

The bonds between the puckered layers of ice are logical locations of gliding. X-ray diffraction patterns of single ice crystals show that gliding appears to take place along the basal plane (Glen and Perutz, 1954; Steineman, 1954). Recently, Kamb (1961) has shown through a thoughtful investigation of previous material and a detailed argument that this is the only logical direction of glide.

Tertiary creep of single ice crystals occurs only after a strain of 10 to 20 per cent (Steinemann, 1954) (See Figure 8). X-ray diffraction patterns show that asterism (smearing of spots) does not increase appreciably until the crystal is subjected to strains over 10 per cent (Glen and Perutz, 1954). Kamb (1961) concludes that the bonds between the layers become broken after large strains and gliding takes place at a higher rate.

Much discussion has been devoted to the creep curve of ice. Although there exists a large amount of data on the subject, it is to some extent contradictory. The observed behavior of ice in creep is best presented by considering the different stages of creep. Results on single ice crystals and polycrystalline samples are presented so that comparisons can be made between them.

#### Primary Creep

Jellinek and Brill (1956) investigated creep of single

ice crystals and polycrystalline ice in tension. Aware that high stresses would produce necking in their specimens (and thereby stress concentrations), they kept their range of stresses between 5 psi and 33 psi. By removing the load from a sample in the second stage (minimum creep rate), they found that the initial elastic recovery was of the same magnitude as the initial elastic deformation. Since total recovery was not possible, they concluded that during load application not only elastic deformation but plastic flow occurs.

If this plastic flow was considered to be linear with time, they found it could be represented by coefficients of viscosity that were apparently independent of stress. These values also agreed with the viscosity coefficients found from the minimum creep rates. They further concluded, then, that Newtonian flow had occurred.

#### Secondary Creep Stage, The Minimum Rate of Creep

Bulk flow laws have usually been derived for the minimum creep rate of ice. Three basic equations have been used to represent the bulk flow of ice (Butkovich and Landauer, 1959). They are

$$\epsilon = ct^r \dots \dots \dots (1)$$

$$\dot{\gamma} = A \sinh (\tau_0 / \tau) \dots \dots \dots (2)$$

$$\dot{\epsilon} = k \tau^n \dots \dots \dots (3a)$$

or

$$\dot{\gamma} = k \tau^n \dots \dots \dots (3b)$$

Jellinek and Brill (1956) and Griggs and Coles (1954) use

a fourth form combining the features of equations 1 and 3a as

$$\epsilon = a \sigma^n t^m \dots \dots \dots (4)$$

The first equation predicts a linearity of log strain versus log time;  $r$  represents the slope of the line in such a plot. Butkovich and Landauer (1959) point out that a creep law of this form is at best only a rough approximation, as stress level plays a major role in the flow of ice. Equation 2 is not recommended by Butkovich and Landauer (1959) because it was awkward to handle and did not give a good representation of data. Equations 3a and 3b assume a linear relationship between time and strain. In the past, most investigators have preferred these forms to represent the creep of ice under low stress. Butkovich and Landauer (1959) investigated all four equations and found that equation 3b best suited the results of 160 specimens.

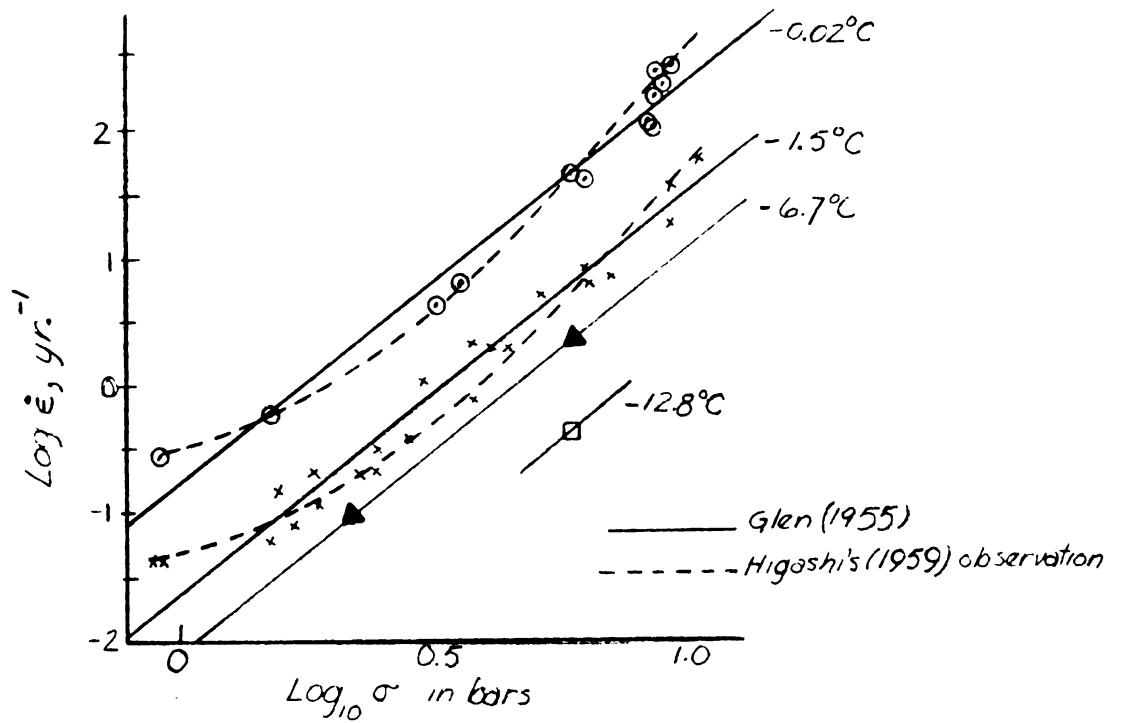
Glen (1955) carried out compression experiments on polycrystalline ice in a stress range from 10 psi to 134.8 psi, studying the steady-state creep rates over long periods of time (100 hours or more). He found that (see Figure 7) by plotting the logarithm of the minimum compressive strain rate,  $\dot{\epsilon}$ , against the logarithm of stress,  $\sigma$ , a nearly straight line was produced for each temperature inspected. As long as the temperature was near the melting point the value of  $n$  (Eq. 3a) had a value of 3.17. At lower temperatures  $n$  became 4.2

Steinemann (1954) performed tests in a Baush Apparatus which allowed direct shear to be placed on his single ice crystals. Since ice glides along its basal plane, he felt that shear and shear rate (equation 3b) would produce the most reliable results. His analysis was like that of Glen (1955) and he found  $n$  to have a mean value of 3.2, comparable to Glen's results (see Figure 7).

The constant  $k$ , according to Glen (1955, 1958) varies with the temperature. It will not affect the rates of straining ( $\dot{\epsilon}$  and  $\dot{\gamma}$ ), but it will affect the magnitude of the strain. Steinemann (1954) believes values of  $k$  will be dependent on stress.

Butkovich and Landauer (1959) using numerous flow data on polycrystalline ice, found  $n = 2.96$  for Eq. 3b. Although their strain rate became apparent only under a log strain log time plot (a contradiction to Eq. 3b), their results were best represented using this form. On single ice crystals they found  $n = 2.5$ .

The cause for variation between flow laws for polycrystalline ice as compared to single ice crystals is not known exactly. Steinemann (1954) expects that the value of  $n$  will be comparable, and that variations in the magnitude of  $k$  will account for the differences. Butkovich and Landauer (1959), on the other hand, believe that the variation in polycrystalline ice is because deformations are not occurring on the basal gliding planes of individual ice



Polycrystalline Ice (Glen, 1955)

Variation of Minimum Creep Rate With Compressive Stress

Figure 7

crystals, but rather at the grain boundaries.

Higashi (1959) found that the minimum creep rate was not proportional to a constant power of stress. From his results of experiments measuring the plastic deformation of hollow ice cylinders subjected to hydrostatic pressure, he concludes that  $n$  in Eq. 3a and 3b is an increasing function of stress. In scrutinizing Glen's (1955) results, Higashi (1959) found the same behavior (see Figure 7). Jellinek and Brill (1956) found serious discrepancies between their work and that of Glen (1955). They felt that Glen's results should correspond to plastic flow, the differences, they explain, are probably due to the methods of testing (tension versus compression; smaller stresses versus higher stresses).

Jellinek and Brill (1956) base their viscoelastic analysis on results which fit Eq. 4. Several relationships become apparent upon inspection of Eq. 4, as follows:

A series of creep experiments conducted at different stress levels allows the isolation of time by plotting strain values versus stress at constant times. This is called the techniques of variable isolation.

The exponent of the time variable,  $m$ , can be obtained by allowing a function of stress and strain to become a parameter in itself. This is accomplished by dividing the strain by the stress raised to the  $n$ th power

and plotting the logarithms of  $\epsilon/\sigma^n$  versus the logarithm of time.  $m$  will be the slope of such a line.

Jellinek and Brill (1956) found that their stress-strain curve drawn in this fashion produced a series of straight lines, i.e., the exponent  $n$  was equal to one. Another series showed this plot to be curvilinear, and when replotted on log-log paper a value of  $n = 1.4$  was obtained.<sup>1</sup>

They found  $m$  to be approximately 0.47 for both series of experiments.

Glen (1955) also used a form similar to Eq. 4. He analyzed his creep curves by assuming that they fit Andrade's Law. Although the results were scattered, he found that the exponent of time would have a value of approximately  $1/3$  (see note in Table 1).

Griggs and Coles (1954) performed compression tests on single ice crystals and found progressively accelerating creep. Their empirical relationship also includes the difference in temperature from  $0^\circ\text{C}$ , as follows:

$$\epsilon = a \left[ (\sigma - bT_0^2) t \right]^2 \dots \dots \dots (5)$$

For a constant temperature this reduces to a form similar to Eq. 3a, or

---

<sup>1</sup>A linear proportionality must exist between stress, strain, and time for a viscoelastic analysis. Jellinek and Brill used the portion of their second curve that was nearly linear.

TABLE 1

SUMMARY OF PREVIOUS INVESTIGATIONS OF SECONDARY CREEP

Investigator	Glen (1952)	Glen (1955)	Steinemann (1954)	Griggs and Coles (1954)	Butkovich and Landauer (1959)	Jellinek (1956)
Type Test	tension cylinders	compression cylinders	pure shear	compression cylinders	shear	tension cylinders
Crystal	poly.	poly.	single	single	single poly.	poly.
Temp. Range	-1.5°C	-0.02°C to -12.8°C	-2.3°C	-10°C	-4°C to -6.5°C	-4.5°C to -15°C
Stress Range	10 to 130 ( $\sigma$ )	10 to 135 ( $\sigma$ )	6 to 31 ( $\tau$ )	10 to 76psi ( $\sigma$ )	6.5 to 140 psi ( $\tau$ )	5 to 33 ( $\sigma$ )
Bulk Flow Equation	3a	3a 4*	3b	4	3b	4
Exponents	n = 4	n = 3.2 to 4.2	n = 2.3 to 4	n = 2 m = 3	n = 2.5 m = 2.96	n = 1 & 1.4 m = 0.47
Duration of Test	140 hrs.+	100 hrs.+	20 hrs.	6 hrs.	16 hrs.+	1 hr.

\* Glen (1955) used an equation based on Andrade's Law which relates stress, strain, and time. If strain is small, it can be expressed as a sum of two terms, one proportional to  $t^{1/3}$  and the other proportional to  $t$ . Results of his analysis were scattered, but using  $t^{1/3}$  gave fair representation. The exponent of stress, n, was found to be 4.2. Butkovich and Landauer (1960) attempted to use this technique of analysis, also. They found it did not work.

$$\epsilon = a\sigma^*{}^2 t^2$$

$$\sigma^* = \sigma - bt_0^2 \quad .$$

Their work was performed over a relatively short period of time, which Glen (1958) feels is responsible for the lack of a uniform flow rate.

A summary of the results of the different investigators is in Table 1. The variables which influence their results include:

- 1) Tension creep versus compression creep
- 2) Shear stress versus compressive stress
- 3) Polycrystalline ice versus single ice crystals
- 4) Stress level
- 5) Duration of loading.

In light of Jellinek's (1957) findings, where physical behavior apparently is highly dependent upon the imperfections in the crystal lattice, it follows that local microscopic deformations would not have a pronounced effect on polycrystalline ice. Properly mounted, compression and tensile polycrystalline samples should produce comparable results.

### Tertiary Creep

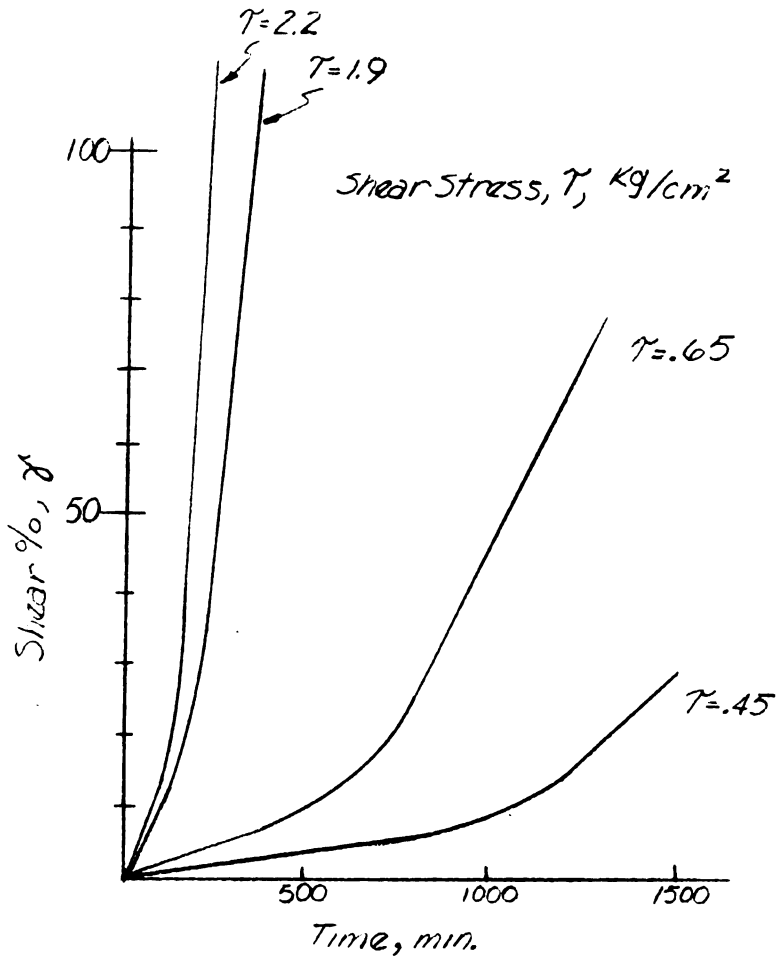
Steinemann (1954) observed tertiary creep in single ice crystals and referred to it as "softening" of the crystal. He is the only investigator to date to calculate a bulk flow for tertiary creep ( $n = 1.5$ ), although most investigators have

observed it. His results are shown in Figure 8. Glen (1958) points out that in compression, tertiary behavior was observed at stresses higher than  $4 \text{ kg/cm}^2$  (57 psi).

Previous investigators (Glen and Perutz, 1954; Jellinek and Brill, 1956; Glen, 1955, 1958; Butkovich and Landauer, 1959; Kamb, 1961) have hinted that tertiary creep occurs after the bonds between the individual crystals have broken. In polycrystalline metals the grain (or crystal) boundaries represent a concentration of dislocations, imperfections in the crystal lattice structure (Finnie and Heller, 1959). When the polycrystals are subjected to large strains, stress concentrations occur at the many grain boundaries and voids begin to open. Creep results (where slower rates facilitate observation of intergranular failure) have shown that the interstitials (extra atoms in the atomic lattice work) migrate to these voids. Eventually a point is reached where slippage between the crystals is excessive, macroscopically defining the ultimate strength of the material. Finnie and Heller (1959) suggest that tertiary creep may begin at this point.

#### Activation Energy of Ice

The atomic structure of materials may be disturbed and distorted by a very small amount of energy, in fact, much less than that of the bonds holding the molecules together. To bring about a disturbance so that a distortion will occur requires an amount of energy called the activation



Single Ice Crystals (Steinemann, 1954)

Variation of Creep With Shear Stress

Figure 8

energy,  $\Delta H$  (Finnie and Heller, 1959). Rates of chemical reaction and physical behavior of engineering materials are governed by the activation energy criterion, which is highly dependent upon the temperature of the material.

Many investigators have shown that the creep rate of a material is governed by activation energy, as follows

$$\dot{\epsilon} = A e^{-\Delta H/RT} \dots \dots \dots (6)$$

where  $R$  is the gas constant,  $T$  is the absolute temperature,  $A$  is a constant, and  $e$  is the base of natural logarithms. Investigators of nickle and aluminum have indicated that the activation energy for these metals is dependent upon the stress level, leading to

$$\dot{\epsilon} = A e^{-\Delta H+f(\sigma)/RT} \dots \dots \dots (7)$$

where " $f(\sigma)$ " means function of stress. Activation energy is usually expressed as calories per gram mole of a system.

On a semilog plot, the log of creep strain rate versus the reciprocal of the absolute temperature will show a nearly linear relationship. The energy of activation for this viscous flow,  $\Delta H$ , can be determined from the slope of the curve within a particular temperature range (Jastrzebski, 1959).

As may be seen from Table 2, investigators find an activation energy between  $13^k$  cal/mole and  $37^k$  cal/mole for ice. Glen (1955) reports a value of  $31.8^k$  cal/mole.

Landauer (1951) points out that this value is strongly dependent upon the use of one creep specimen at  $-12.8^{\circ}\text{C}$ , and a liberal error could be present in the value. Landauer

TABLE 2  
ACTIVATION ENERGY OF ICE

Investigator	Specimen	Test Type	Temp. Range	Activation Energy k cal/mole
Glen, J.W. (1955)	poly. ice	compression	1.5 to 12.8	31.8
Jellinek and Brill (1956)	poly. ice	tension	5 to 15	16.1
Landauer (1957)*	snow	compression	3.6 to 13.55	14 to 27
Nakaya (1959)	commercial ice	sonic	5 to 30	12.7
Nakaya (1959)	superimposed ice	sonic	5 to 30	13.5
Nakaya (1959)	ice with elongated bubbles	sonic	5 to 30	13.9
Nakaya (1959)	ice with small bubbles	sonic	5 to 30	18.7
Higashi, A. (1959)	commercial ice	hollow cylinders under hydrostatic pressure	1.9 and 10.8	37.8

\*Snow does not have steady flow; values are based on assumption that equilibrium flow has been reached.

(1957) did not disprove Glen's (1955) value, as he was attempting to relate the activation energy of snow to ice. For snow  $\Delta H$  varies from  $14^k$  cal/mole to  $27^k$  cal/mole. Higashi's (1959)  $37.8^k$  cal/mole is the highest value reported. He bases this value upon three tests.<sup>1</sup>

Nakaya (1959), by observing the damping in oscillograms of ice, has developed a technique of measuring the viscosity of ice. Viscosity can be related to shear flow, which in turn serves as a basis to compute the activation energy. He finds that different types of ice do not have a large variation in their activation energies, but their respective Young's moduli vary over a large range. Jellinek and Brill's (1956)  $\Delta H$  agrees well with the results of Nakaya (1959).

Referring to Higashi's (1959) statement that the value of  $n$  in equation 3a should increase with stress, and to equation 7, it is interesting to note that the activation energy of ice may be a function of stress. If this were the case, the behavior observed by Griggs and Coles (1954), Glen (1955) (as interpreted by Higashi, 1959), and Higashi (1959), could be explained. Both Higashi (1959) and Glen (1955) determined the activation energy of ice from experiments

---

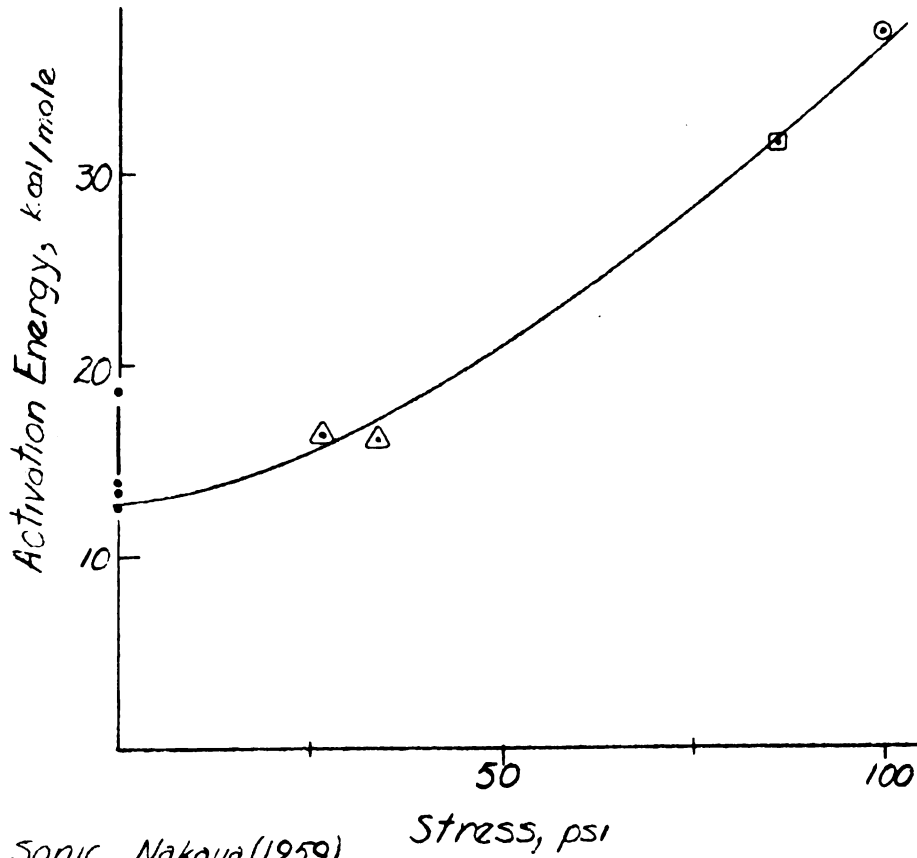
<sup>1</sup>Higashi's results are based on three samples, each at 100 psi confining pressure. The straight line used to determine  $\Delta H$  is the "average" of these samples. Assuming one sample was incorrect, activation energies could be calculated ranging from 4 k cal/mole to 124 k cal/mole.

conducted at relatively large stress levels; their results are comparable. The values of  $\Delta H$  determined at low stress levels (Jellinek and Brill, 1956) are comparable to the values based on the sonic technique (Nakaya, 1959).

Equations 3a and 6 should be related in some fashion, since they both represent minimum creep rate. Figure 9 shows the activation energies found by the investigators of ice, compared to the stress level for which each value was obtained. Nakaya's (1959) sonic tests were assumed to be representative of the lower bound (creep under no load). From this figure  $\Delta H$  appears to be based on some function of stress. Since this value will be an exponent in Eq. 7, and since both Eq. 7 and Eq. 3a represent  $\dot{\epsilon}$ , Higashi's conclusion concerning equation 3a is supported.

#### Effect of Confining Pressure on Creep

Very little work has been performed on ice under confinement. Rigsby's (1958) experiments are the most notable to date. By applying pressure to a single crystal of ice under pure shear he was able to study the deformation rates under varying confining pressures. Results of his experiments (Figure 10a) show that at a constant temperature, the rate of deformation increased with the application of pressure. His apparatus was capable of immense confining pressures (1 atmosphere to 306 atmospheres). His conclusions are based on the results of four specimens.



- Sonic, Nakaya (1959)
- △ 27-34 psi, Jellinek and Brill (1956)
- 87 psi, Glan (1955)
- 100 psi, Higashi (1959)

Variation of the Activation Energy of Ice With Stress

Figure 9

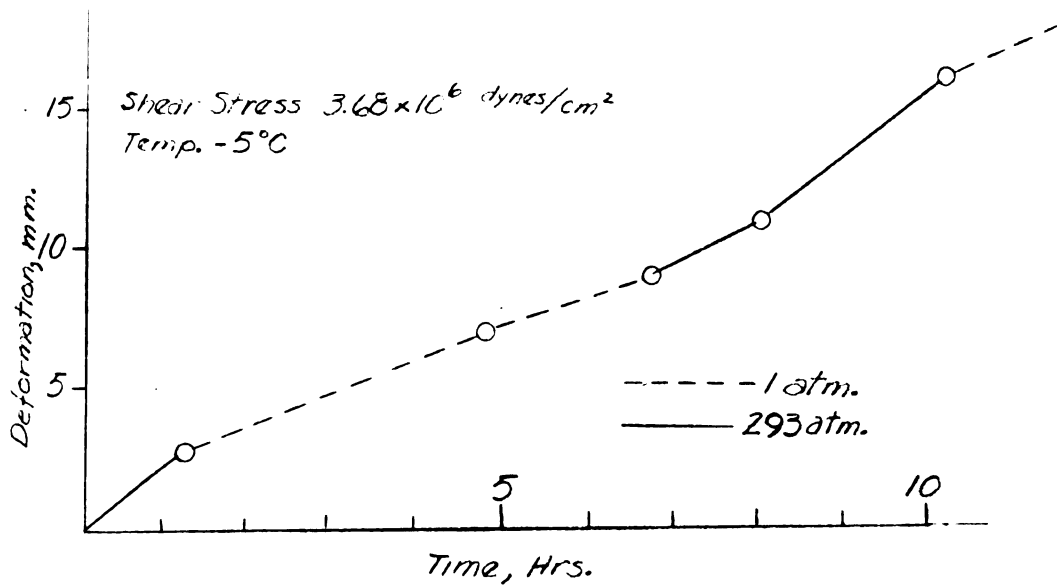
Realizing that confining pressure has an effect upon the melting point of ice, he became curious as to the effect of pressure upon deformation rate when the difference in temperature between the sample and melting point of the sample was held constant (Figure 10b). His conclusions are

. . . that the shear strain rate for plastic deformation of single ice crystals deforming by gliding on the basal glide planes is practically independent of hydrostatic pressure when the difference between ice temperature and melting point is maintained at a constant interval.

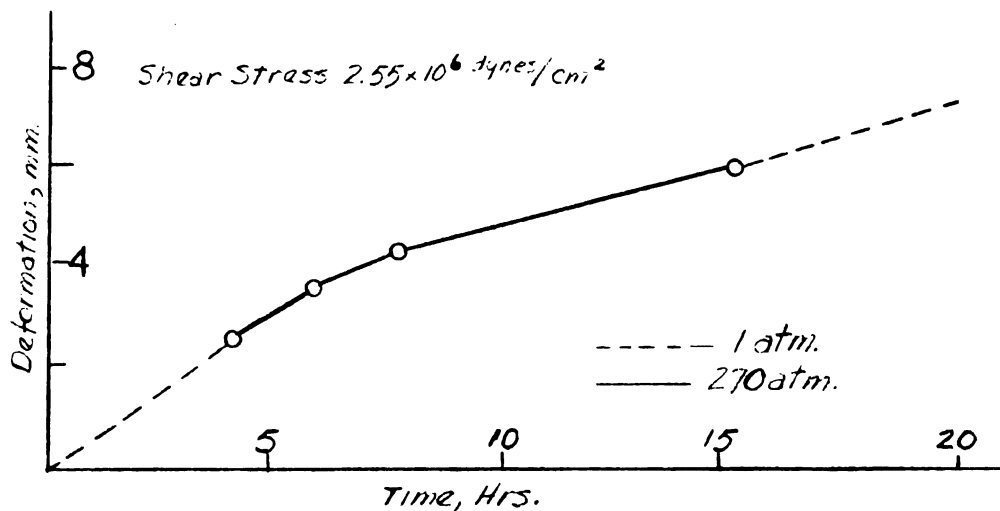
#### Viscoelastic Properties of Ice

Viscoelastic deformation is the result of the combined action of a material's elastic and viscous elements when subjected to applied forces (Jastrzebski, 1959). Since real materials are neither ideal liquids (viscous) nor ideal solids (elastic), the last decade has seen increased acceptance of viscoelastic models to represent the behavior of engineering materials. In their simplest form, they are composed of springs representing the elastic elements and dashpots representing the viscous elements. These elements are combined into various series and parallel configurations to produce mathematical expressions for stress-strain-time relationships which may suit a given material under study (Secor and Monismith, 1961). The simplest models are those of Voigt, Maxwell, and Burger. Their configurations are shown in Figure 11a.

The Maxwell model is composed of a spring and a dashpot in series, having an elastic element,  $E_1$ , and a



Deformation vs. Time at Varying Hydrostatic Pressure  
Figure 10a



Deformation vs Time at Varying Hydrostatic Pressure.  
Constant Temperature Difference Between Ice Temp. and Melting Point approx.  $3^\circ\text{C}$

Figure 10b

Single Ice Crystals (Rigsby, 1958)

Influence of Confining Pressure on Creep

Figure 10

viscous element,  $\eta_1$ . The Voigt model is composed of a spring and dashpot in parallel, having elements of  $E_2$  and  $\eta_2$ , respectively. The Burgers model is a combination of the Maxwell model and the Voigt model. Where  $\sigma$  is the stress,  $\epsilon$  the strain, and  $t$  the time, the behavior of the Voigt model can be shown to be

$$\sigma(t) = E_2 \epsilon(t) + \eta_2 \frac{d\epsilon(t)}{dt} .$$

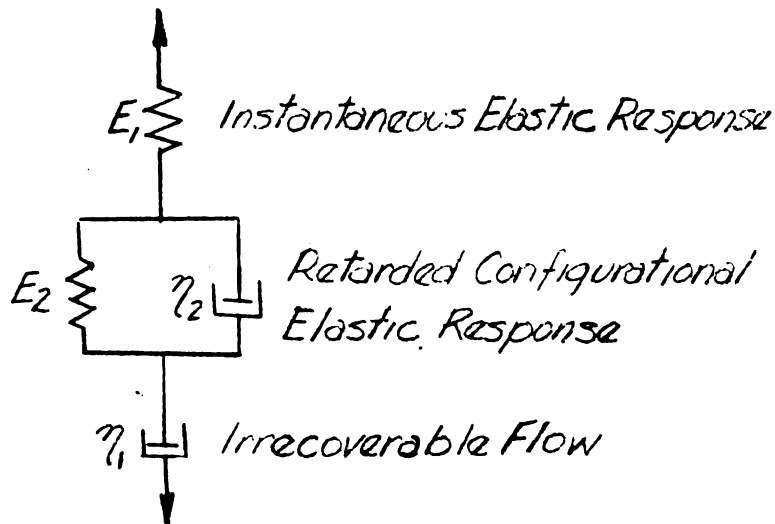
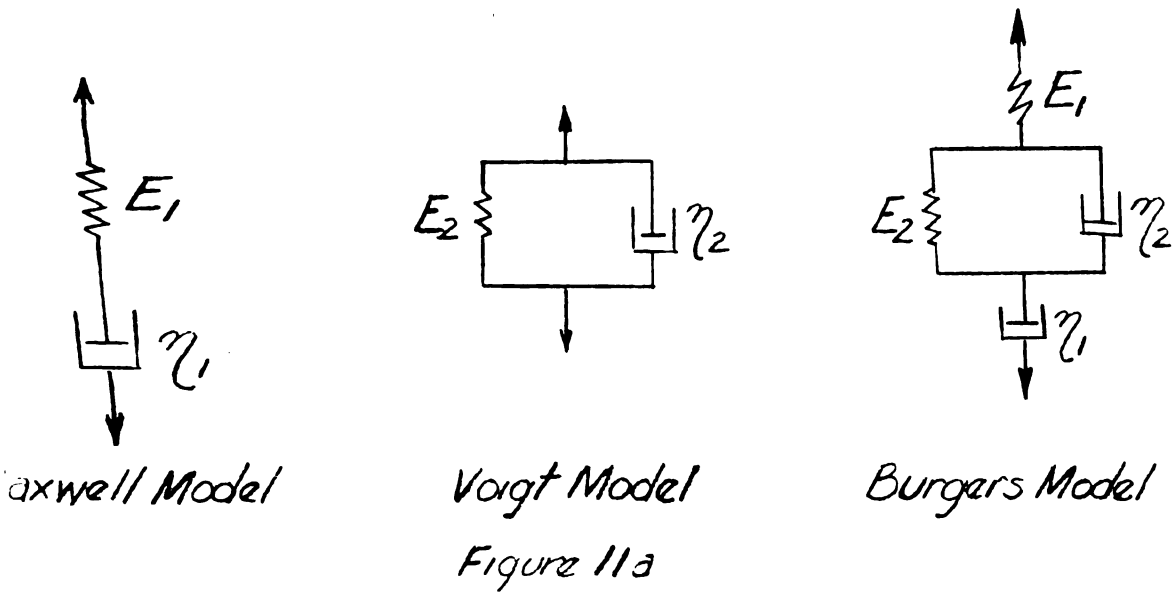
The differential equation for the Maxwell model is

$$\frac{d\epsilon(t)}{dt} = \frac{1}{\eta_1} \sigma(t) + \frac{1}{E_1} \frac{d\sigma(t)}{dt}$$

A very important step in the understanding of viscoelastic models was taken by Boltzman in 1878, in which he related the behavior of a material to its past history. According to this theory, the strain at any time due to a variable load history is given by the sum of the strain contributions from each past instant (Finnie and Heller, 1959). This principle of superposition allows the behavior of the Burgers model to be represented by the sum of the behavior of a Maxwell model and a Voigt model. The mathematical expression for strain of a Burgers model is as follows

$$\epsilon = \frac{\sigma}{E_1} + \frac{\sigma t}{\eta_1} + \frac{\sigma}{E_2} (1 - e^{-t/T_{ret}}) . . (8)$$

The retardation time,  $T_{ret}$ , can be closely approximated by its relationships to the elements of the Voigt model,  $\eta_2$ ,



Mechanical Model of the Threefold Response of a Polymer to Applied Stress  
Figure 11b

Basic Viscoelastic Models

Figure 11

$E_2$ , and Poisson's ratio  $\mu$ , (Jellinek and Brill, 1956, as

$$\gamma_{2/E_2} = \frac{T_{ret}}{2(1+\mu)}$$

The attempt to give physical significance to the various elements of a viscoelastic model has been difficult in the past. However, Goldman (1957) does present an idealized Burgers model, assigning specific behavior to the several elements of the model for an amorphous polymer (Figure 11b).

His three categories are as follows:

1. A rapid, reversible elastic response (characterized by a high modulus).
2. Configurational elasticity associated with the straightening out and orientation of the polymer chains. This response is characterized by a low modulus of elasticity and is time-dependent, being retarded by the internal viscosity of the medium.
3. The irrecoverable slippage of entire polymer chains past each other. This is the true viscous flow, and is characterized by the melt viscosity of the polymer, the feature persisting at higher temperatures.

These categories are dependent primarily upon the chemical composition, molecular architecture, and temperature of the medium. Viscoelastic materials are usually so complex that no simple model will determine their behavior, and the models must be modified by adding many Voigt models in series or parallel.

Since the degree of complexity of observed behavior of viscoelastic materials is astronomic, in the last few years investigators have been in search of a series of simple tests

which will provide sufficient information to determine the kind of model to represent the behavior and the magnitudes of the elements in these various models.

The tests commonly used today are creep under constant load, relaxation at a given strain, creep followed by removal of the load, stress-strain tests with a constant-rate-of-stress-application, and determination of Young's modulus by resonant frequency. Several of these tests are described in the following paragraphs, which explain how previous investigators have used them to evaluate the elements of the models.

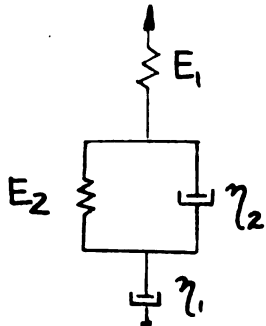
Nakaya (1959) assumed a Maxwell model for his study in which the dashpot's coefficient of viscosity was determined from the damping of the vibrations produced in the test specimens. The viscosity, he observed, increased in an exponential form with a decrease in temperature.

Jellinek and Brill (1956) successfully used a Burgers model to predict the creep and relaxation of ice under low stress conditions. Spring  $E_1$  should represent the instantaneous elastic response of ice (Goldman, 1957) (see Figure 12 and 13c). Jellinek and Brill (1956) determined the value of this spring from the instantaneous deformation of a polycrystalline specimen just after the load has been applied (see Figure 13). Their value for  $E_1$  was 814,000 psi<sup>1</sup>, lower than the value for an ice of comparable density (1,060,000 psi)

---

<sup>1</sup>The value used by Jellinek and Brill (1956) represents the average of values ranging from 320,000 psi to 1,120,000 psi.

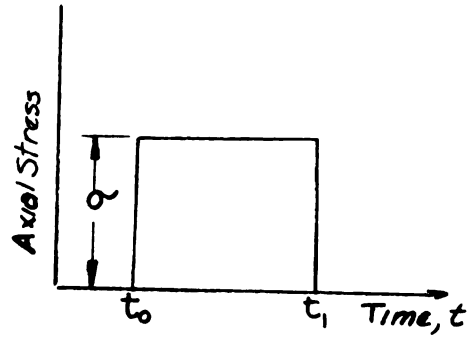
11



Burgers Model

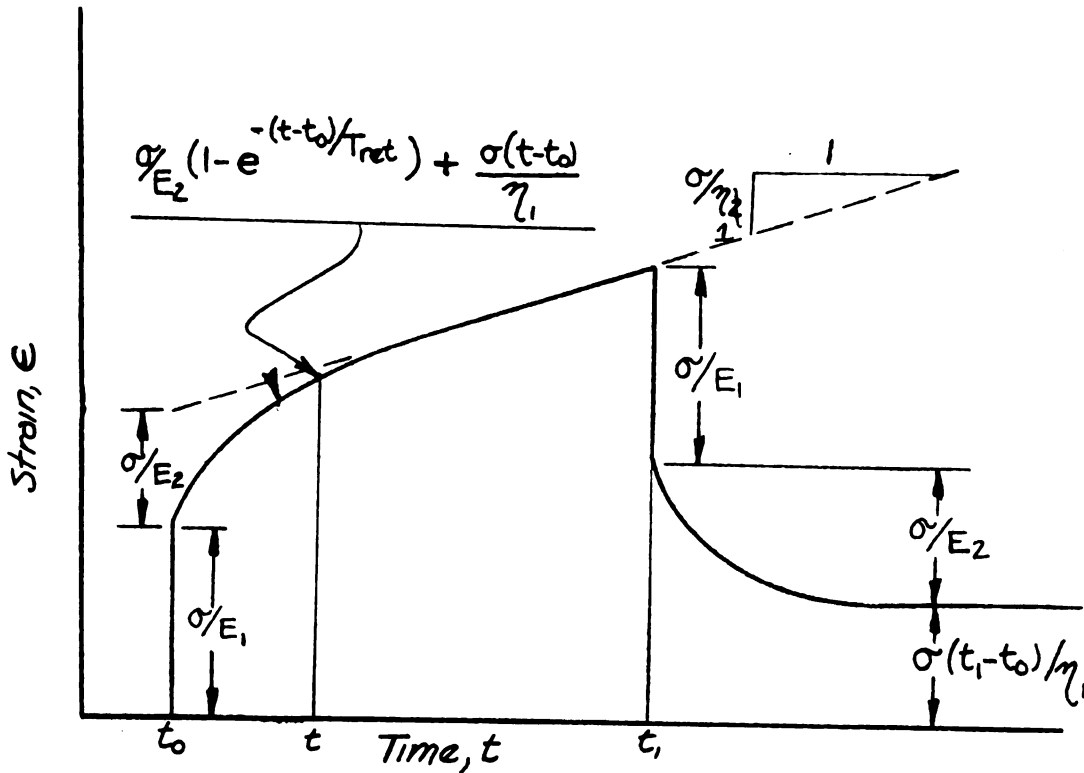
$$\epsilon_{\text{VOLT}} = \frac{\sigma}{E_2} (1 - e^{-t/T_{\text{ret}}})$$

Figure 13a



Load History

Figure 13b



Strain-Time Curve

Figure 13c

Behavior of a Burgers Model In Creep and Relaxation

Figure 12

as given by Nakaya, (1959).

The value of  $E_1$  may also be obtained from the recovered strain observed when the load is suddenly removed from a creeping specimen. The instantaneous recovery strain (the vertical straight line in Fig. 13b) has a magnitude of  $\sigma/E_1$ . Jellinek and Brill (1956) found that their values of  $E_1$  determined in this manner agreed reasonably with those found by the method described in the preceding paragraph.

The bulk flow laws of ice which consider time as a parameter represent viscoelastic flow. The viscous elements,  $\eta_1$  and  $\eta_2$ , of a Burgers model are time dependent.  $\eta_1$  is best calculated from a relaxation curve as shown in Figure 13c.  $\eta_2$  is best calculated from the slope of the "steady state flow," the minimum creep rate (Jellinek and Brill, 1956; Finnie and Heller, 1959; Secor and Monismith, 1961).

Values of the viscous elements in a Burgers model can be checked by comparing the measured strains in the primary creep stage (transition zone) to the strains predicted by the Burgers model in primary creep (Jellinek and Brill, 1956). The mathematical expression for strain of a Burgers model in primary creep is

$$\epsilon = \sigma/E_2 (1 - e^{-\Delta t/T_{ret}}) + \frac{\sigma \Delta t}{\eta_1} .$$

Both  $\eta_1$  and  $\eta_2$  are distorting in primary creep (see Fig. 13c).

The elements of the Voigt model were determined from the curved portion of the creep curve in Jellinek and Brill's (1956) analysis. There was extremely good agreement between the viscous elements found in this manner and those found from the deformation recovery curves observed after the load had been removed from creeping specimens.

The value of spring  $E_2$  may be determined either from a creep curve or a relaxation curve. The strain found by projecting the slope of the secondary creep stage back to the initial deformation axis will allow a strain to be extrapolated which is  $\sigma/E_2$  in magnitude. From a relaxation curve this same value of strain,  $\sigma/E_2$ , can be taken from the curve as shown in Figure 12c. The elastic element  $E_2$ , determined by Jellinek and Brill (1956) apparently increases in magnitude as the temperature decreases.

Density of ice has a pronounced effect upon the viscous elements  $\eta_1$  and  $\eta_2$  (Nakaya, 1959). An ice having a density less than pure ice<sup>1</sup> will produce a creep curve showing higher rates of creep and larger deformations, i.e., its Burgers model elements would have smaller viscous elements.

The viscous element  $\eta_1$ , can be related to the activation energy as follows (Jellinek and Brill, 1956):

$$\eta_1 = \text{const } e^{-\Delta H/RT}$$

---

<sup>1</sup>Low density ice usually has a large degree of trapped air bubbles in it.

It should be reemphasized that Jellinek and Brill's (1956) analysis is based on a linear stress-strain-time relationship, i.e. Boltzman's principle of superposition is valid. Recent investigations into the viscoelastic behavior of textile fibers (Finnie and Heller, 1959) show that a basic stress-strain relationship, such as Eq. 8, can be used even for non-linear responses. In this case the stress must be raised to a power larger than one.

Most engineering materials show deviations from linearity both in the elastic and viscous range, and their behavior can be better approximated by the equation:

$$\epsilon_t = \frac{\sigma}{E} + A \sigma^\alpha (1 - e^{-qt}) + B \sigma^n t \dots (9)$$

Where A, B, q, n, and d are constant characteristics for each material under specific conditions and must be determined from experiments. It should be noted that these constants, although they have no real rheological meaning, correspond to the rheological coefficients in the equation for the behavior of the Burgers model. Thus A becomes related to  $1/E_2$ , q to  $1/T_{ret}$ , and B to  $1/\eta_1$ .  $\alpha$  and n are introduced to account for the deviations from linearity (Van Vlack, 1959).

The intuitive feeling for viscoelastic behavior obtained from a simple model is one of its chief attributes. A schematic model representing non-linear behavior would be composed of many Voigt and Maxwell models hooked in series

and/or parallel. Such a diagram would be so complex that it would lose its ability to give the investigator this "clairvoyant" sensation he so desires.

An understanding of the mechanical properties of ice is necessary before satisfactory methods for the analysis of a frozen soil can be formulated. As mentioned in the introduction, ice within a frozen soil will be subjected to both high stress and confining pressure, thus the mechanical properties of polycrystalline ice under these conditions should provide a clue to the rheological behavior of frozen soil. In this study, creep experiments and constant rate of strain experiments have been used to provide some answers to the behavior of polycrystalline ice.

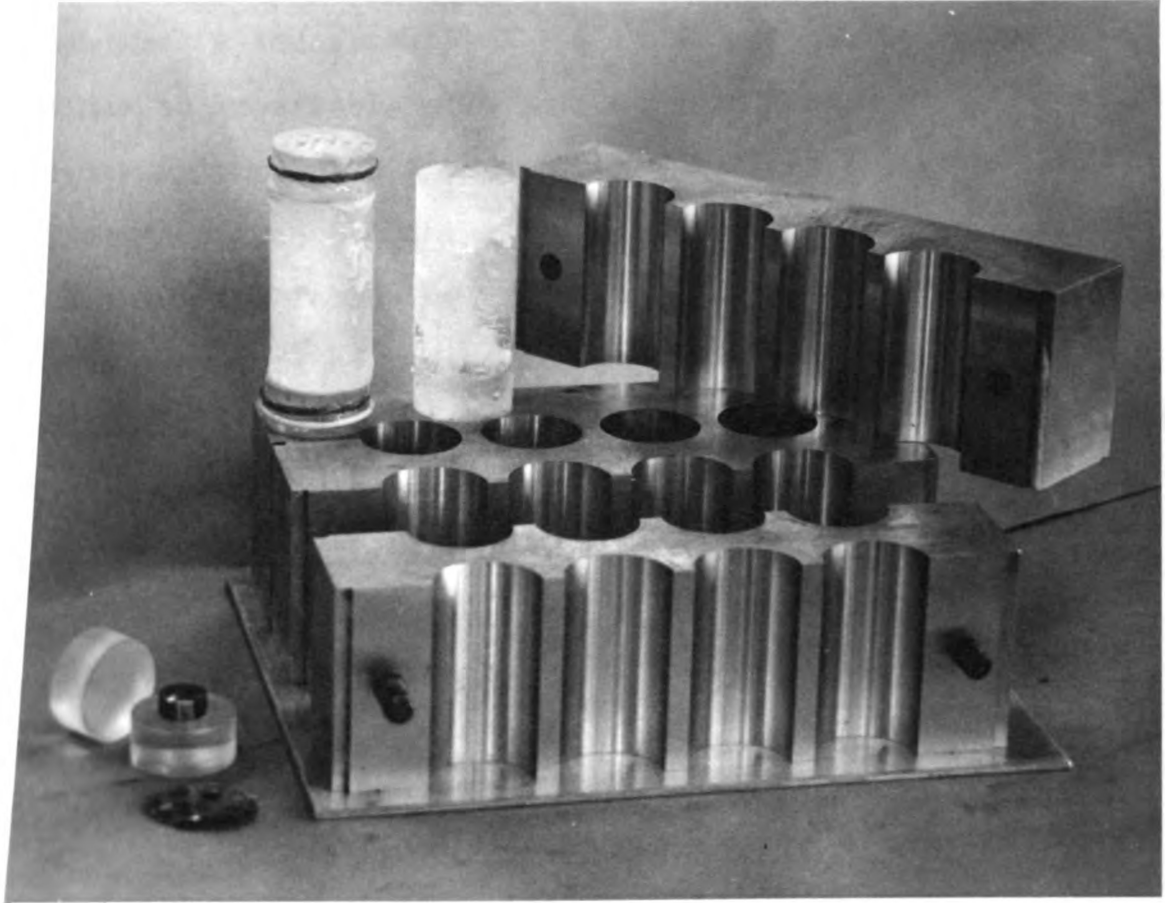
## CHAPTER III

### APPARATUS AND PROCEDURES

The water used in this experiment was distilled and deionized. The water was checked for the amount of dissolved salts with an RD-D4 Solu-Bridge, which indicated that on the average only 1.5 parts per million of dissolved salt were present. All glassware that came in contact with the water was first thoroughly cleaned with a sulfuric acid sodium dichromate cleaning solution. Before using the water it was boiled for at least 1 1/2 hours in a flask to drive off dissolved air. One liter was sufficient to fill the mold.

An aluminum mold similar to that used by Leonards and Andersland (1960) was used to form the ice specimens (see Figure 13). The mold was coated with a thin film of Dow-Corning high-vacuum silicon stop-cock grease to prevent adhesion between the mold and ice. To prevent leakage between the mold and its baseplate, each was coated with grease.

The water and the mold were both at room temperature during the filling of the mold. To prevent small air bubbles from mixing with the water, a 100 ml pipette was used to take the water from the flask and place it in the ice mold. The



Disassembled Aluminum Ice Mold, Specimens,  
and Loading Paraphernalia

Figure 13

filled mold was then placed in a large refrigerator box which maintained a temperature of  $-18^{\circ} \pm 1^{\circ} \text{C}$ , and the water was allowed to supercool. The samples were frozen at  $-4^{\circ} \text{C} \pm 1/2^{\circ} \text{C}$  by seeding them with a crystal of distilled deionized ice. Nucleation proceeded through the sample at a moderate rate, and during the following growth the samples were not disturbed. After 12 or more hours the ice mold was taken to another refrigerator box at  $-15^{\circ} \text{C}$ . The mold was kept covered with aluminum foil to prevent evaporation.

The top of the cylindrical samples were trimmed at an age of two or more days with a single-edged razor blade and allowed to remain in the mold until a few days before testing. Any nicks accidentally cut into the tops of the cylinders during trimming were filled with a drop of water and retrimmed.

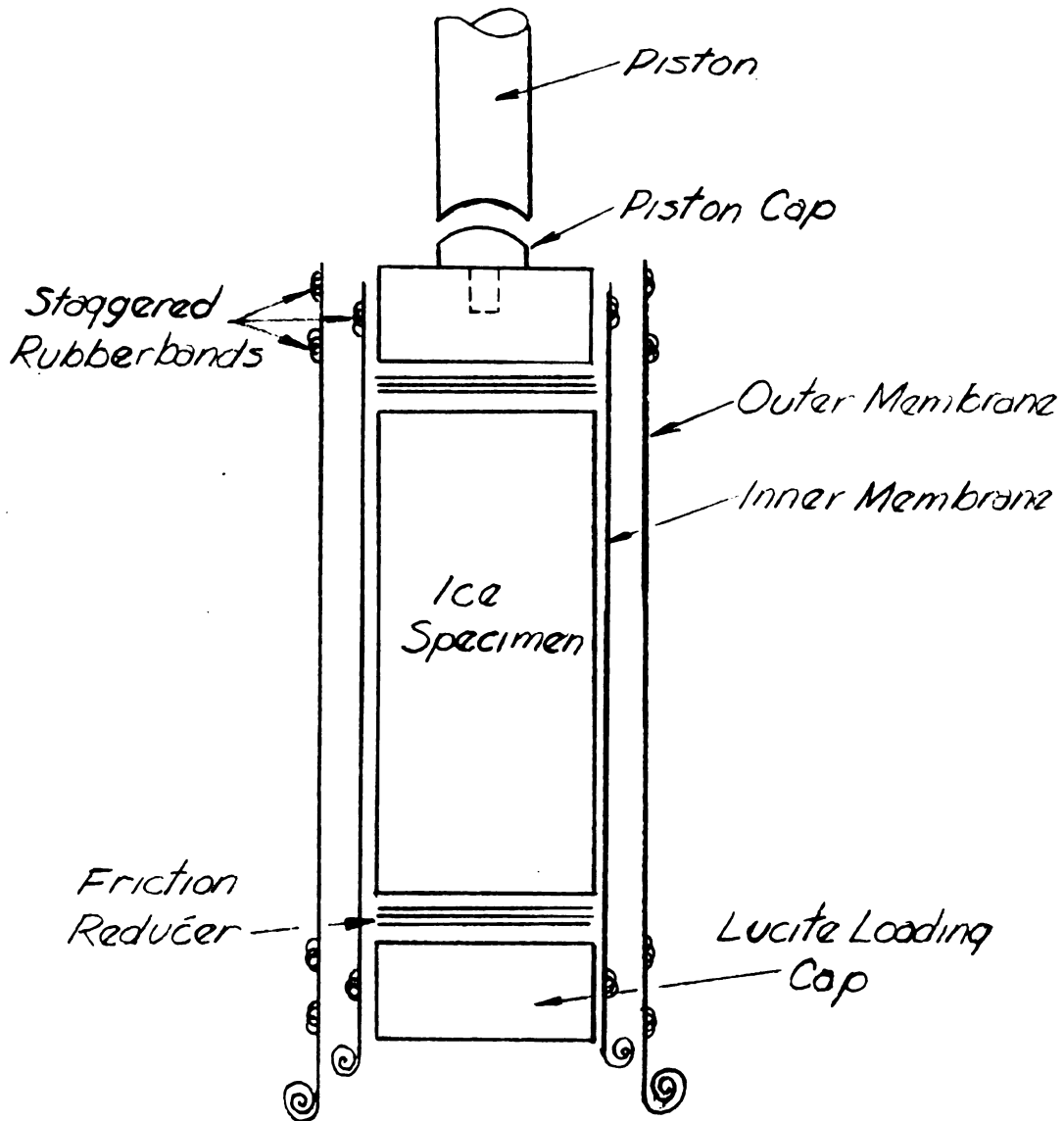
Before the ice specimens were placed in membranes, they were visually inspected for cracks, if such were observed, the specimen was discarded. Bad cracks were uncommon. Specimens prepared in this manner were slightly cloudy. A few small spherical air bubbles could be seen in the samples. Their density did not differ measurably from that of clear ice ( $0.917 \text{ gm/cm}^3$ ). Four batches of ice specimens were made. The last batch made had the lowest density,  $0.915 \text{ gm/cm}^3$ . Specimens from this batch appeared to have more air bubbles trapped in them than in previously prepared samples.

Since Jellinek's (1957) observations that adhesion to loading plates and ice creates stress components in a lateral

direction, a friction reducer was used between the loading cap and ice specimen. Leonards and Andersland (1960) used thin hard rubber discs to reduce friction, while Butkovich (1954) used chamois or sponge rubber.

The friction reducer selected consists of a three-layered "sandwich," the top and bottom of which are thin polyethylene plastic sheets and the middle layer is a perforated sheet of aluminum foil (Serata, 1961). Holding these pieces together is a viscous mixture of stop-cock grease and finely powdered graphite. Perforations in the aluminum foil (quarter inch holes made with a paper punch) provide small reservoirs of grease and graphite, preventing the unit from working as one piece. Serata (1961) found that these friction reducers work extremely well even under high pressures (9,000 psi). The friction reducers are pre-compressed to drive out surplus grease by placing them between two metal plates and compressing them with a Universal testing machine. These "sandwiches" may be used several times.

Since only a small amount of ethylene glycol (even vapor) is sufficient to greatly alter the strength characteristics of ice, it is imperative that the ice samples are isolated from the cooling bath. Furthermore, evaporation of the ice can be quite pronounced if the samples are not isolated from the air (Glen, 1955). Glen (1955) tested his



Schematic Diagram of an Ice Specimen  
Prepared for Testing

Figure 14

creep specimens by immersing them in a paraffin bath. Specimens used in these tests were not exposed to the atmosphere more than a few minutes.

Figure 15 shows schematically how the specimens were jacketed in membranes, how the loading caps and friction reducers were placed, and how rubber bands were staggered so that leakage between the membranes and the specimen was impossible. A hole was provided in the top loading cap to seat a removable steel piston cap.

A Tinius Olson Universal Testing Machine with a load holding device was used for all tests conducted. The main hydraulic system may be diverted through a small needle valve, which allows more accurate control on the hydraulic system of the loading head, hence control on the movement of the loading head. It was possible to pre-set this valve, causing the moving head to move at a prescribed rate. Setting this rate immediately before a test was conducted (allowing the hydraulic system to come to equilibrium) insured a given rate of deformation of the loading head. It was found that the resistance given by the test sample was not sufficient to alter the constant movement of the loading head. This technique was used to produce the data for the constant-rate-of-strain tests.

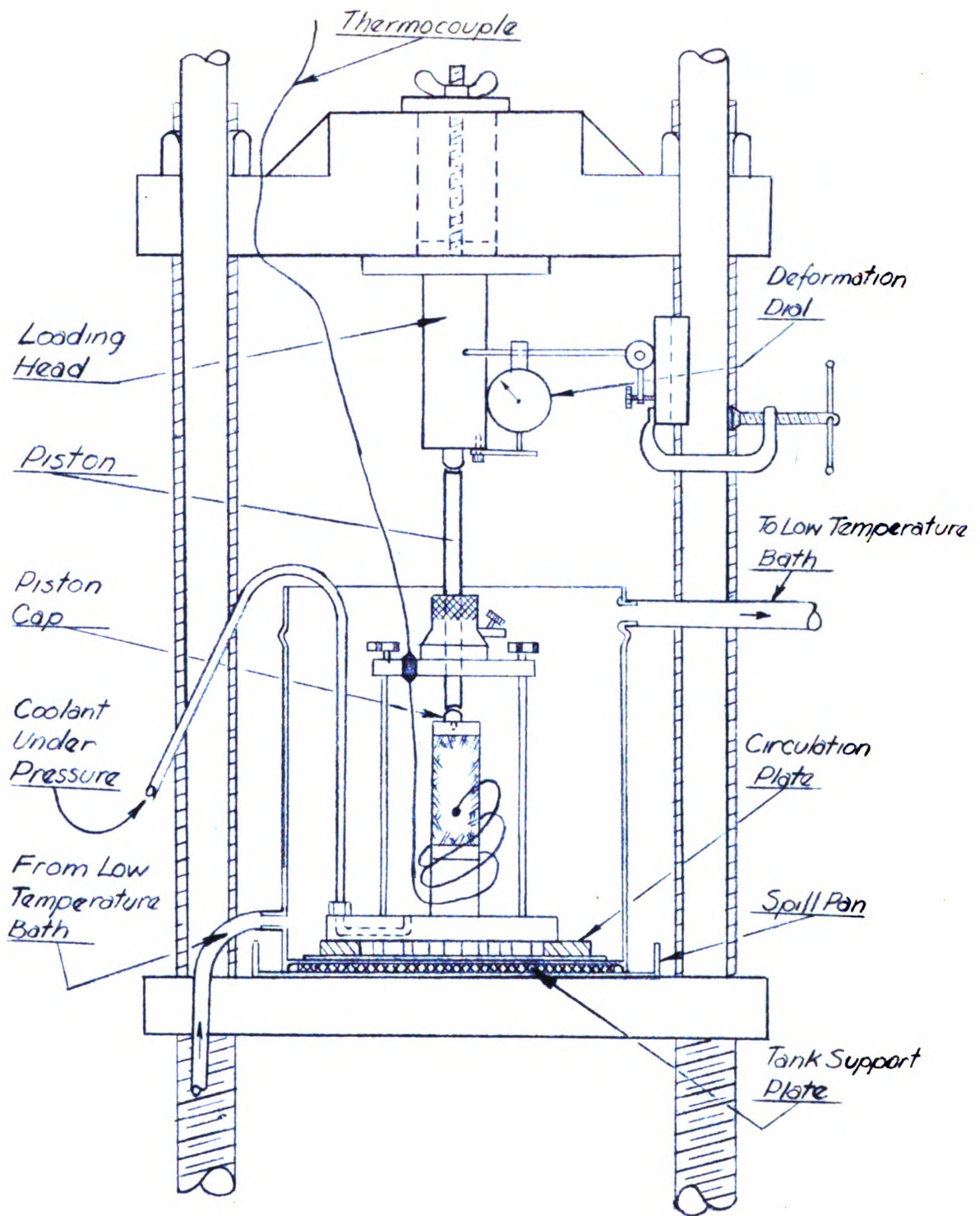
For the constant-rate-of-strain experiments loads were read from the load dial at given intervals of time by marking the position of the indicator on the glass dial with

a grease pencil. The deformation reading at the end of the test was compared to the total time over which the test was conducted. It was found that the predicted deformation and actual deformation agreed within  $\pm 0.0005$  inches for the total time of test.

Also connected to this needle valve is the load holding device. A desired load may be "fixed" on the loading dial by locking a pointer arm at the desired load. When the moving load-indicator arm touches the fixed pointer a circuit is completed and the needle valve closes, causing a drop in hydraulic pressure and a reduction in load. When the moving indicator arm is no longer in contact with the fixed arm, the circuit is again open, and hydraulic pressure is re-applied to the loading head.

This technique was used to obtain the creep data. It was observed that the load varied, on the average of less than  $\pm 2$  pounds. In the case of creep at a very high load level, it was found that the load was hard to hold as it had a tendency to drop off. A variation of  $\pm 5$  lbs. was observed. For this large a variation it was assumed that the sample had failed.

Deformation of the sample was measured relative to the loading head as compared to the base of the testing machine. Measurements were read to the nearest 0.0005 inch. Time was measured to the nearest second with a Lab-chron Timer.



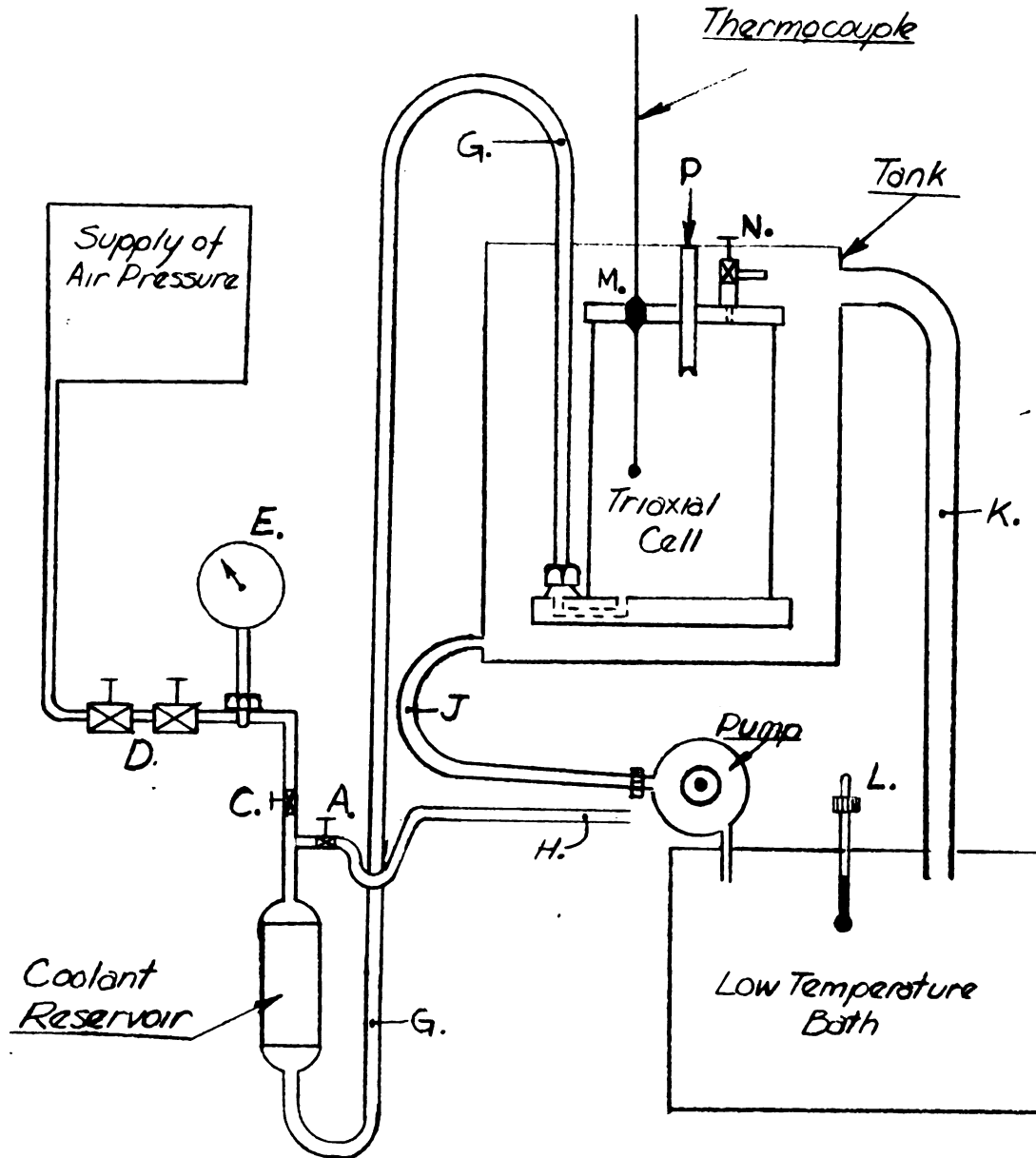
## Test Equipment

Figure 15

A triaxial cell was used as a test cell. It was modified in order that a thermocouple could be passed through the cell and attached to the surface of the sample. This was accomplished by tapping a hole in the metal cell top and inserting a brass fitting so sealed that it would not leak when the cell was under pressure. Figure 15 shows how the test cell was placed in the testing equipment. To place the specimen in the cell, a technique was developed in the course of the experimentation which exposed the frozen sample to a minimum of warming. The detailed procedure is outlined in the appendix.

The schematic diagram of the pressure system used is shown in Figure 16. The cell was filled by means of the pump on the temperature bath through line HAG, with valve C closed. Stop-cock N was open, allowing the air in the cell to escape. Air pressure was used to supply confining pressure to the sample through line CG with valve A closed. The pressure was controlled by the double valve, D, and measured with the gauge E. The cell could be drained easily by placing it in the coolant bath, opening valves A and N and lifting the cell top from the base plate. When the fluid was under pressure it flowed from line GAH without any additional pressure.

Ethylene glycol containing 50 per cent water by volume was used as a coolant fluid. A pump supplied the coolant to the circulating tank which held the test cell. The tank,



Schematic Diagram of Hydraulic and Cooling System

Figure 16

made from a standard five-gallon can, was constructed so that the coolant entered at the bottom and returned to the bath from a line at the top of the tank. This supply and return of coolant was continuous throughout the period of testing (see Figure 15) and maintained the cell temperature to  $\pm 0.05^{\circ}$  C. The cell was isolated from the bottom of the tank by a circulation plate which allowed the coolant to flow beneath the cell as well as around it. This minimized temperature change by heat conduction through the base.

Since moisture condensed on the outside of the tank, a spill pan was placed under the tank to catch the condensation. This spill pan also caught any coolant that might flow over the sides of the tank when the test cell was placed in the tank, and served as a safety device should the line returning to the bath become inoperative. To prevent errors in deformation readings the test tank was supported by a circular plate placed between the tank and the spill pan.

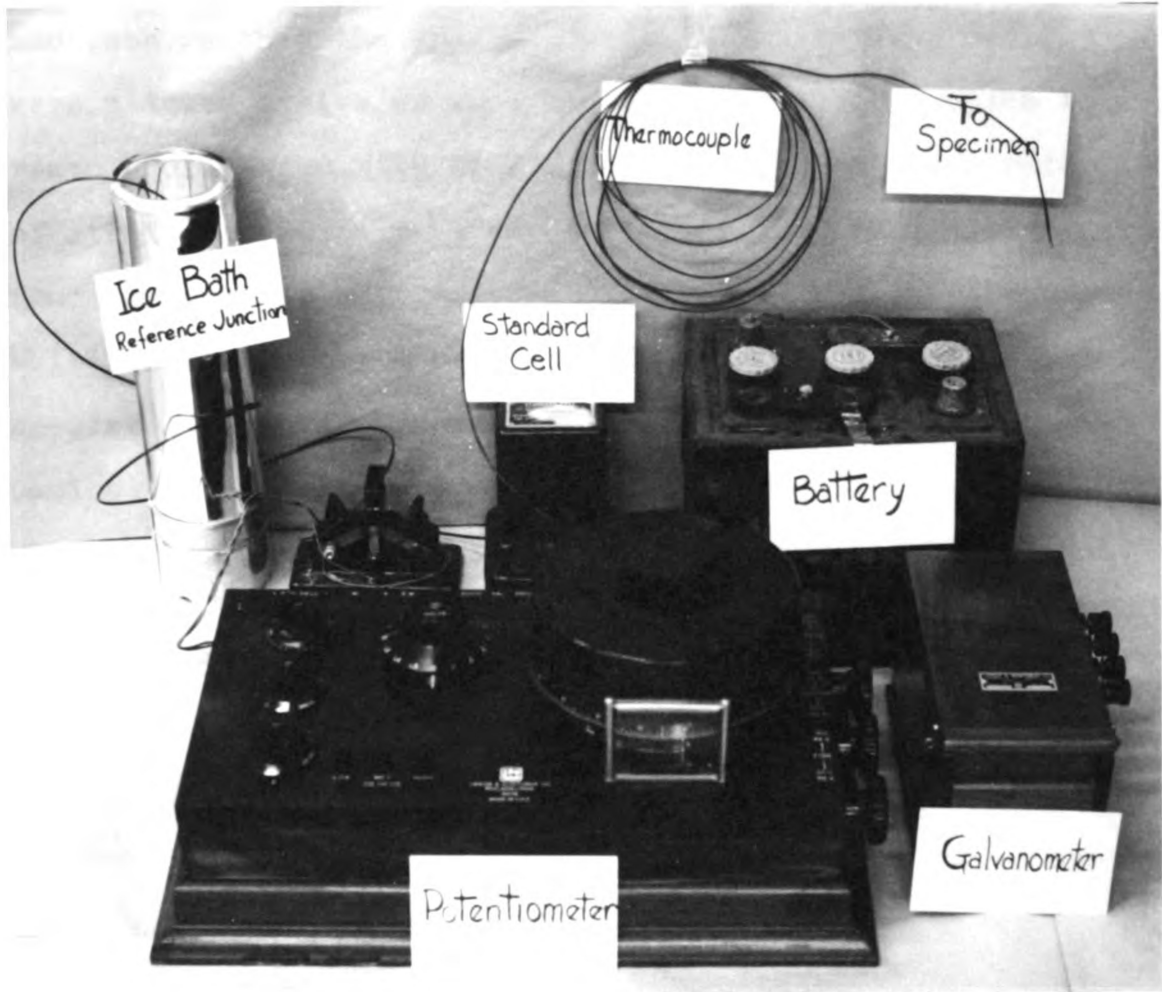
The low temperature bath was controlled by a mercury thermostat submerged in the bath. The temperature difference between the tank and bath was approximately one degree centigrade. Because the temperature did not remain constant within the room it was necessary to change the setting of the thermostat periodically.

The temperature of the sample was obtained by use of a copper-constantan thermocouple (Scott, 1941), and a Leeds and Northrup potentiometer, Model K-2. A bath of distilled

deionized, melting ice was used as a reference temperature. A standard cell (1.0915 volts) and a Leeds and Northrup Galvanometer aided in measurement. These instruments were powered by a standard car battery. The thermocouple arrangement was capable of reading to the nearest  $0.02^{\circ}$  C. The temperature measuring equipment is shown in Figure 17.

Based on the temperatures measured on the surface of specimens, it was found that the cooling system was quite efficient. In the circulating tank the temperature of the entering fluid was  $1/2^{\circ}$  C colder than the temperature of the coolant returning to the source (temperature bath). The coolant in the triaxial cell was not moving and protected the specimens from any temperature variation of the circulating tank. During the time taken to transport the specimens from the cold storage and to mount them on the triaxial cell, the specimens were exposed to room temperature for a short period of time. During the filling of the test cell the temperature of most specimens was  $-9^{\circ} \pm 2^{\circ}$  C. All experiments were conducted at  $-4^{\circ}$  C  $\pm 0.05^{\circ}$  C. Several of the first specimens used cooled to the test temperature after having warmed to  $-3^{\circ}$  C during mounting.

It was found that the frozen samples would reach the test temperature within two and one-half hours. Providing the circulating tank was at the correct temperature level, the temperature at the surface of the specimen remained nearly constant ( $\pm 0.05^{\circ}$  C) indicating thermal equilibrium



Temperature Measuring Equipment

Figure 17

had been reached. To make sure that thermal equilibrium had been reached the specimen and its surrounding coolant were allowed twelve or more hours (overnight) in which to reach equilibrium with each other. A few duplicate rate of strain specimens were exceptions as they were tested four hours after being placed in the test cell. No noticeable difference was observed in the results of these specimens when they were compared to their duplicate companion.

## CHAPTER IV

### EXPERIMENTAL RESULTS AND DISCUSSIONS

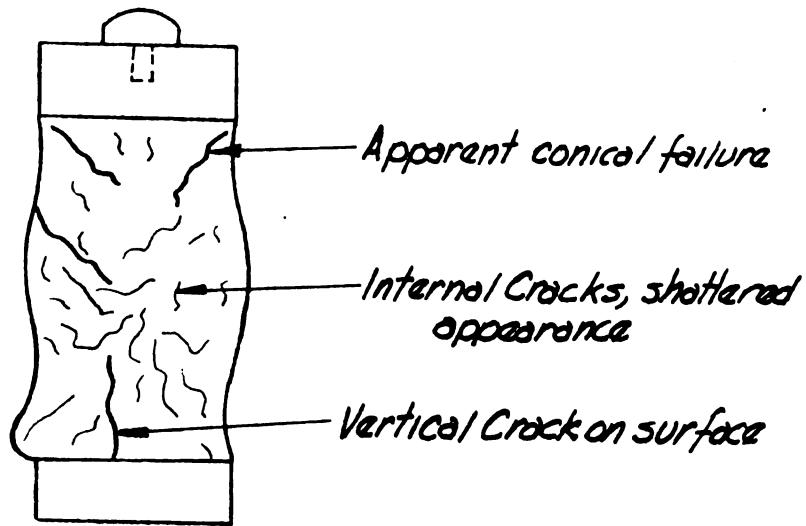
#### Results of Constant Rate of Axial Deformation Experiments

Twenty cylinders of polycrystalline ice were tested under constant rates of axial deformation until failure occurred. Four rates were used, approximately doubling the rate for each series of experiments. The rates used are 0.54%, 0.95%, 1.76% and 3.33% expressed as per cent of axial deformation per minute. Confining pressures of 0 psi, 30 psi and 45 psi were used. All results are summarized in Figures 20a, b, c, and d.

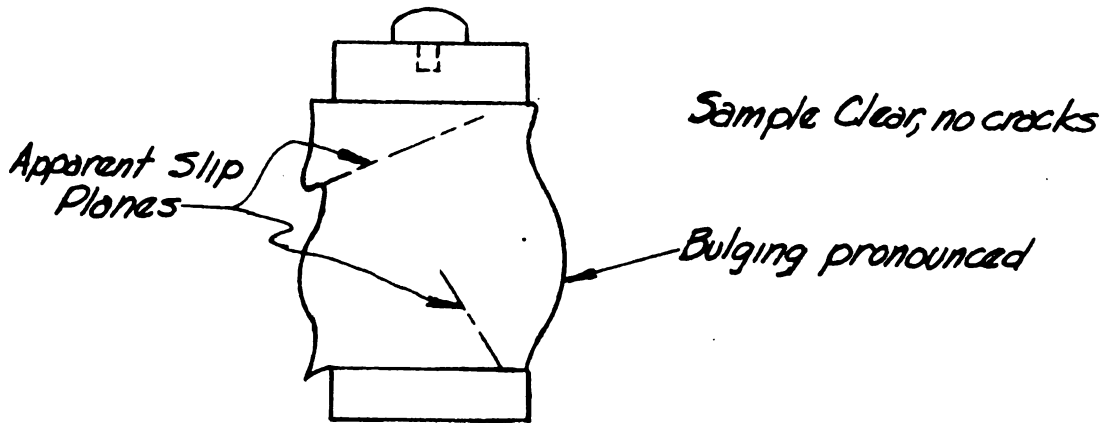
The temperature at the beginning of each experiment was  $-4^{\circ}\text{C} \pm 0.05^{\circ}\text{C}$ . The temperature was checked periodically during the experiment and a trend for the sample to warm was observed. This may be due to the thermal energy created as the specimen deforms.

Experiments performed with the fastest rate of loading required less than two minutes to produce failure of the specimen. For this rate load readings were taken at two second intervals with the help of a timekeeper.

Most of the constant-rate-of-strain specimens that failed had a shattered appearance when taken from the test cell (Butkovich, 1954). A typical failed specimen is sketched in Figure 18.



*Failed Constant-Rate of Strain Specimen, I-12*



*Creep Specimen I-27, Constant Load 300lbs*

*Typical Appearance of Specimens After Testing*

*Figure 18*

In all samples tested there was a time lag before the load indicator responded to the deformation applied to the sample. In soil testing this effect is eliminated when the loading caps are properly seated on the specimen. Several factors may influence the seating strain for the ice samples. They are:

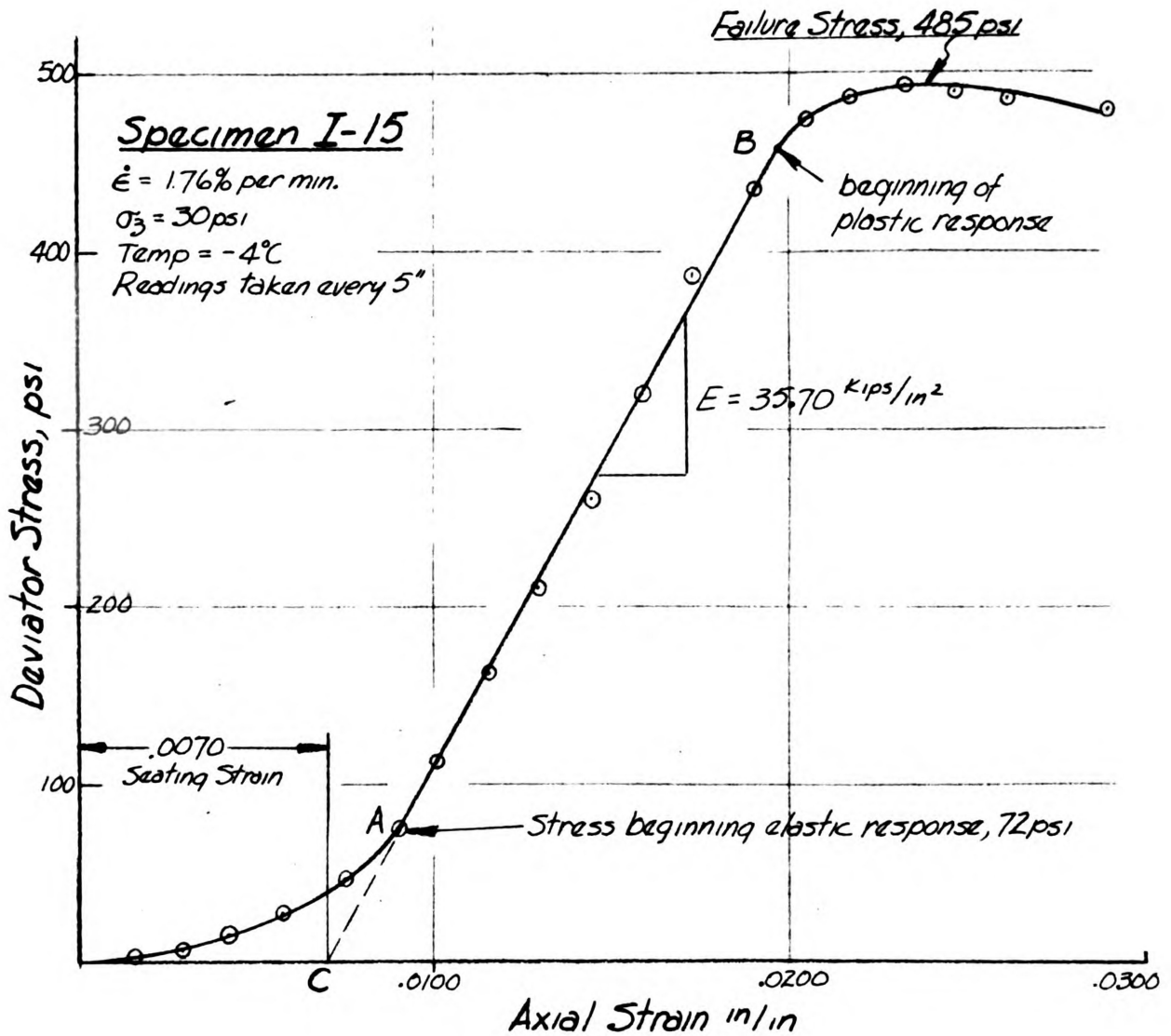
- 1) Compression of the friction reducers
- 2) Response of the lucite loading caps
- 3) Seating of the specimen on the sample mount
- 4) Seating of the loading caps on the specimen.

A typical response of ice to a constant rate of strain is shown in Figure 19. The seating strain is defined as the intercept strain found by prolonging the elastic portion of the stress-strain curve (viz. line AB in Figure 20) to the strain axis. This is shown as point C in Figure 19.

A comparison of the stress at which point A occurred shows that, for a given strain rate (1.76% per minute), ten of fourteen samples began their elastic response between 67 psi and 73 psi. The fourteen samples are composed of six constant-rate-of-strain experiments and eight approach curves for creep. The samples which did not fit into the previously given range of stress began their elastic response at 48 psi, 80 psi, 106 psi and 118 psi. The seating strain, as previously defined, varied from 0.0036 to 0.0081 inches/inch.

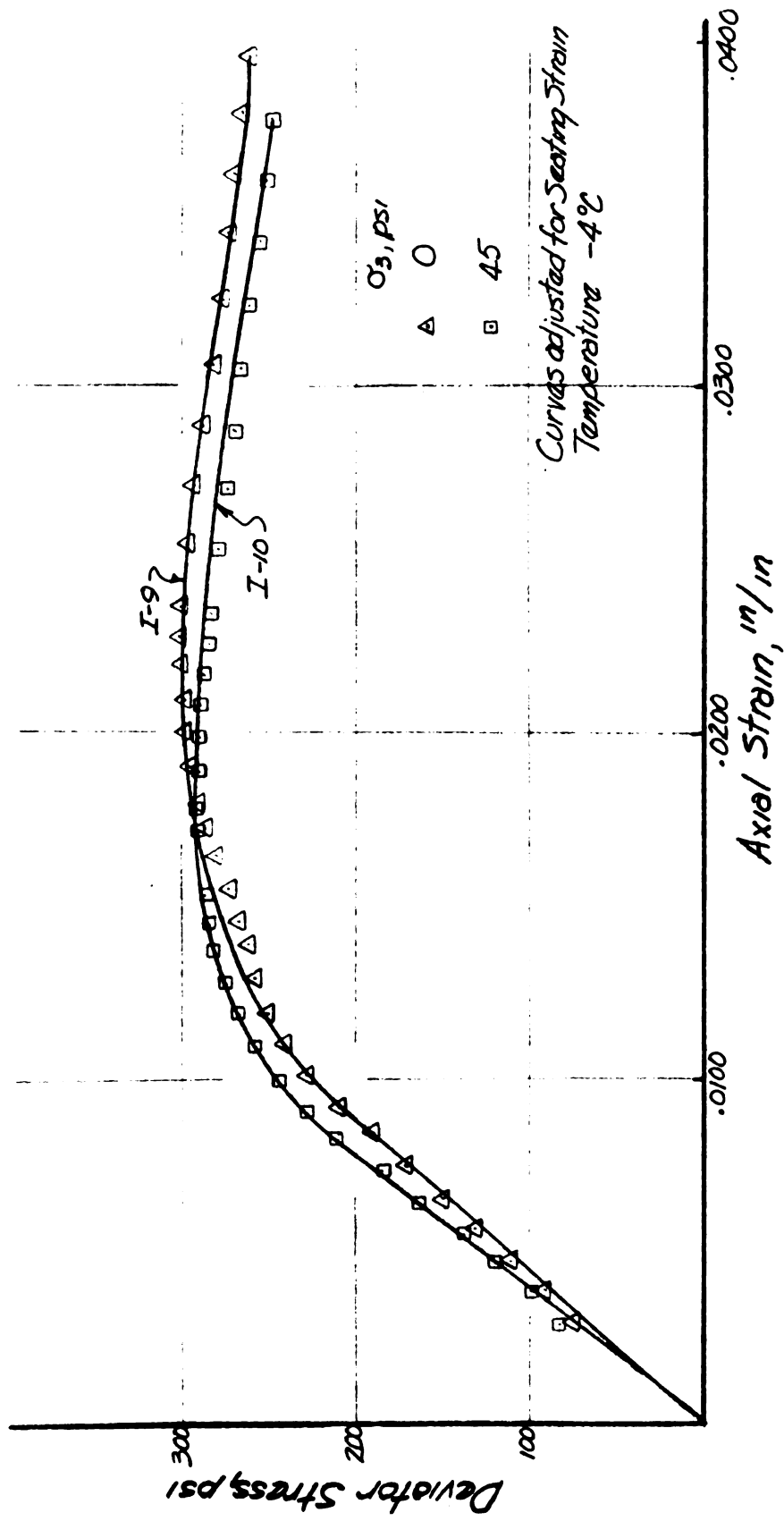
Values of Young's modulus were determined from the stress-strain curves in Figures 21a, b, c and d and are





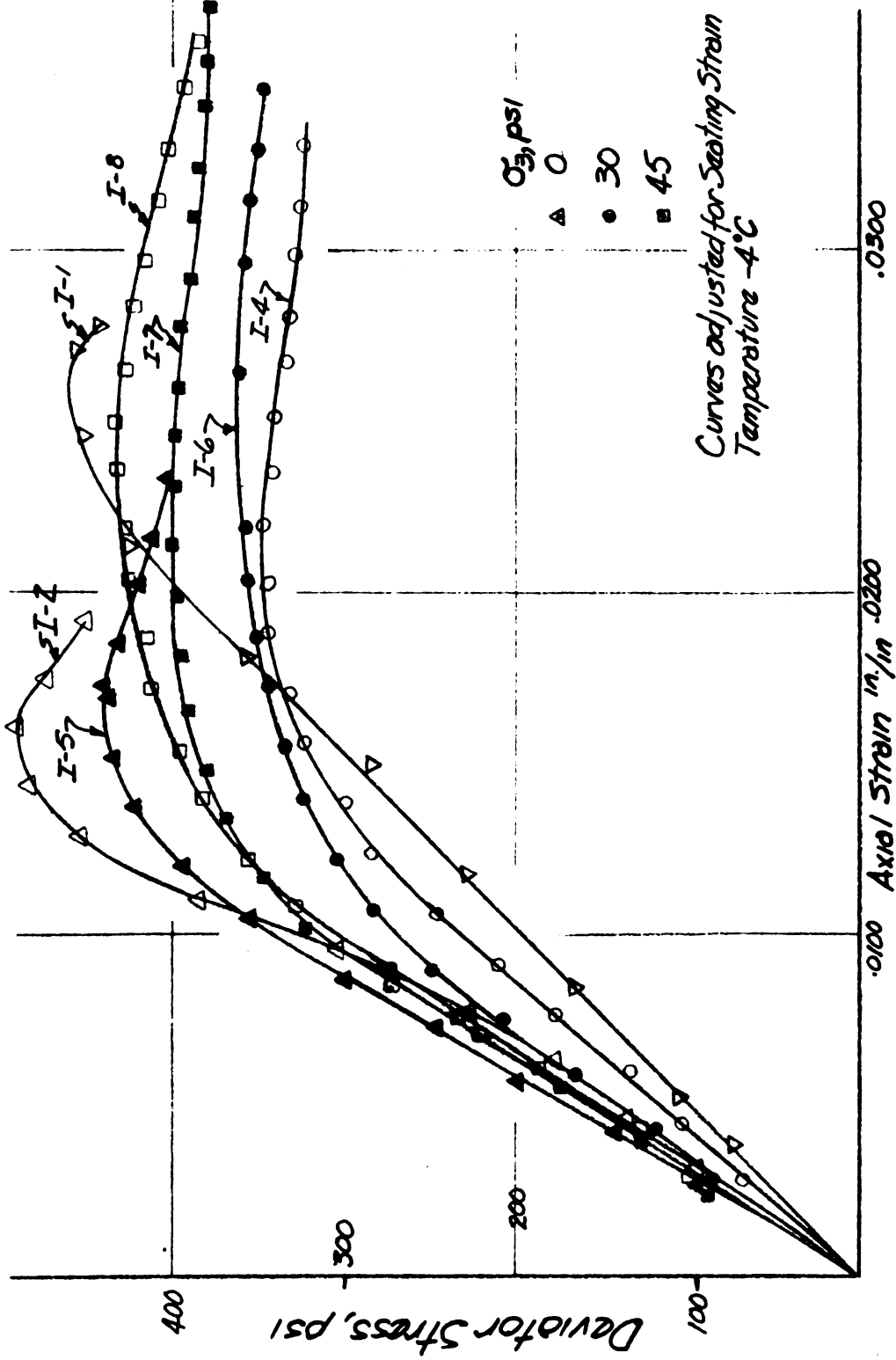
Typical Response of Ice Subjected to A Constant  
Rate of Axial Deformation.

Figure 19

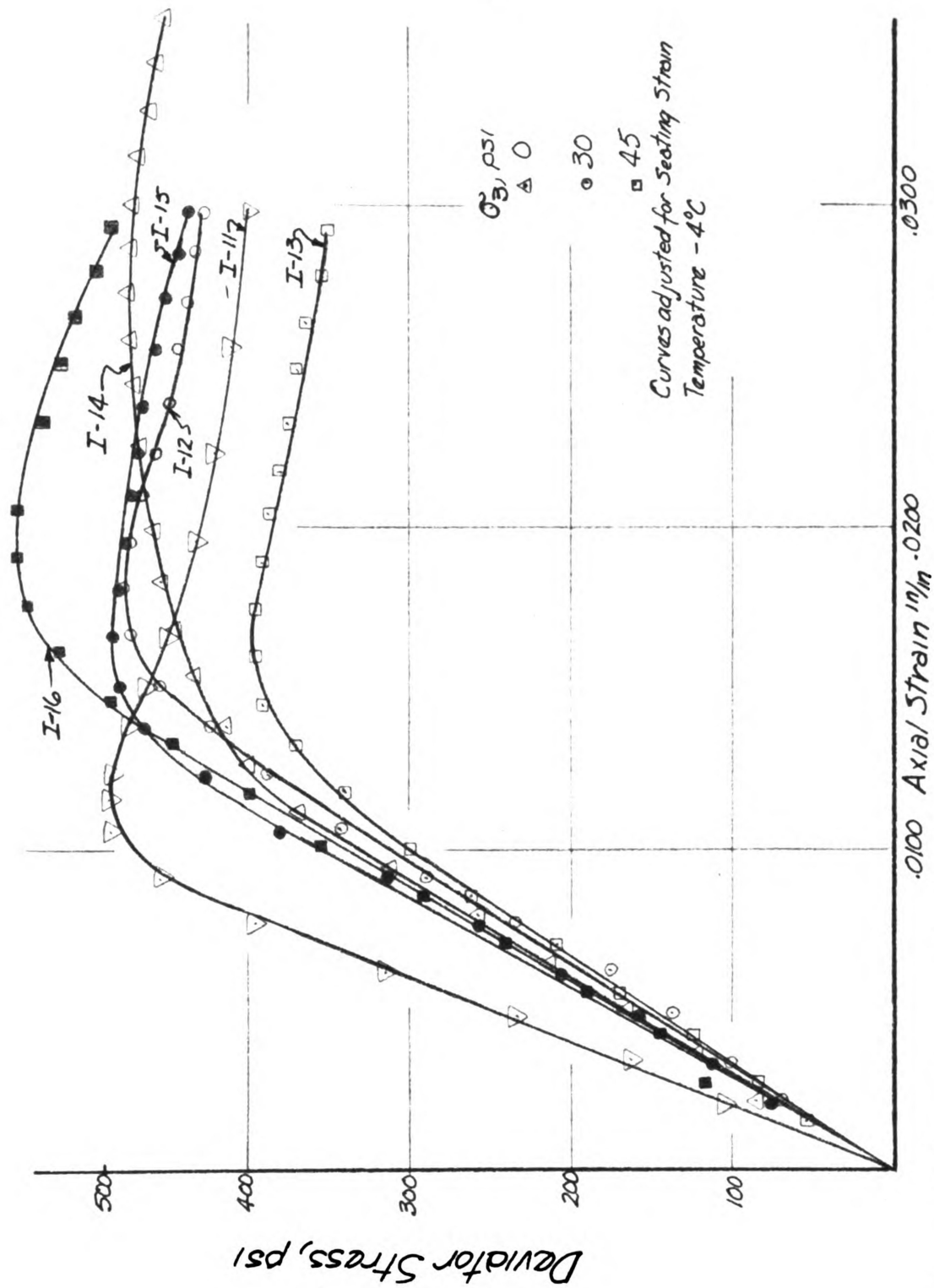


Stress-Strain Curve for Ice  
Rate-of-Strain 0.54% per Minute

Figure 20a

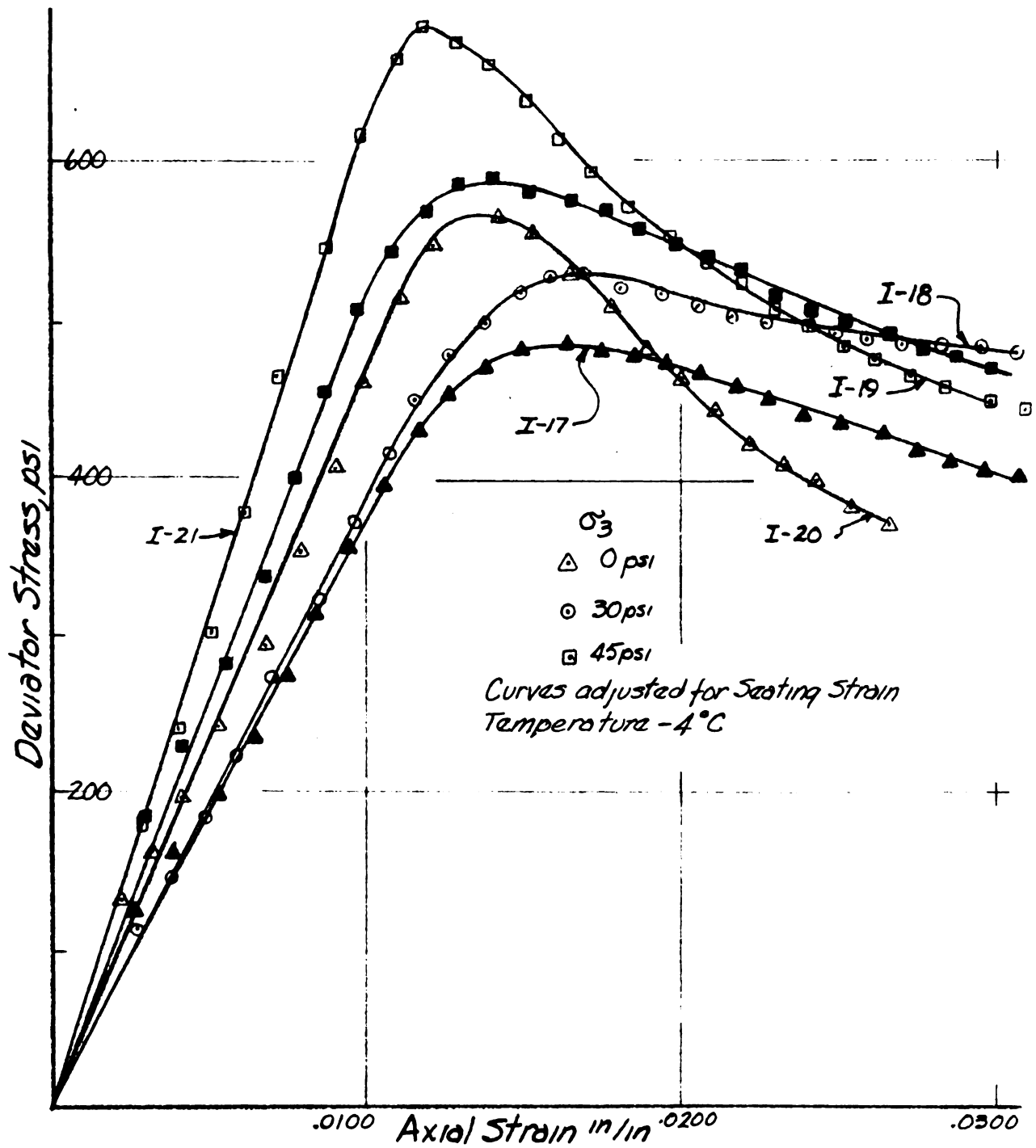


Stress Strain Curve for Ice  
Rate of Strain 0.95 % per Minute  
Figure 20b



Stress Strain Curve for Ica, Rate of Strain 1.76% per Minute

Figure 20c



Stress Strain Curve for Ice  
Rate-of-Strain 3.33% per Minute

Figure 20d

TABLE 3  
SUMMARY OF CONSTANT-RATE-OF-STRAIN RESULTS

Sample	$\dot{\epsilon}, \%$	$\sigma_3, \text{psi}$	E, Kips/in <sup>2</sup>	$\epsilon_p$	$\epsilon_{ult}$	$\sigma_{ult}, \text{psi}$
I - 1	0.95	0	19.62	.0185	.0260	456
I - 2	0.95	0	35.09	.0110	.0160	495
5	0.95	0	35.80	.0105	.0170	439
4	0.95	30	23.52	.0105	.0212	346
6	0.95	30	27.44	.0090	.0265	362
7	0.95	45	31.87	.0096	.0213	400
8	0.95	45	30.27	.0108	.0250	433
9	0.54	0	25.30	.0083	.228	400
10	0.54	45	22.79	.0093	.178	390
11	1.76	0	50.00	.0086	.0118	485
14	1.76	0	32.95	.0112	.0273	473
12	1.76	30	31.65	.0123	.0182	476
15	1.76	30	35.70	.0112	.0166	483
13	1.76	45	30.00	.0100	.0168	398
16	1.76	45	33.70	.0133	.0190	543
17	3.33	0	37.50	.0105	.0162	483
20	3.33	0	46.71	.0110	.0137	565
18	3.33	30	47.29	.0113	.0168	530
19	3.33	45	53.12	.0095	.0140	580
21	3.33	45	65.22	.0096	.0113	685

$\dot{\epsilon}$ , Strain Rate in % per minute

$\sigma_3$ , Confining Pressure

E, Young's Modulus

$\epsilon_p$ , Strain at Beginning of Plastic Response

$\epsilon_{ult}$ , Failure Strain

$\sigma_{ult}$ , Failure Stress.

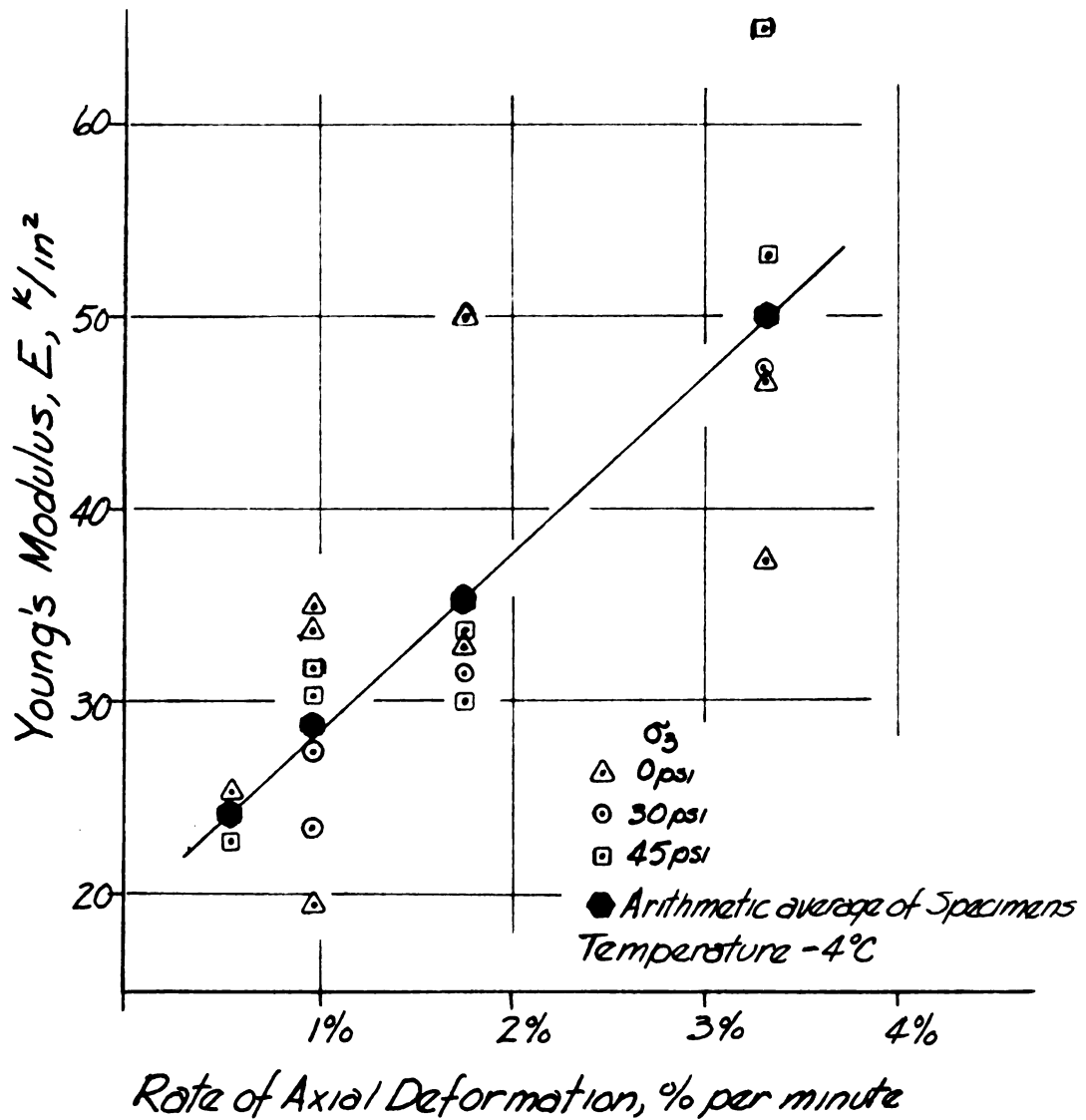
summarized in Table 3. The strains are adjusted for seating strain. Values of Young's modulus determined in this manner show a very definite trend, but vary as much as 20,000 psi

for a given strain rate. The average value for Young's modulus increases as the strain rate increases. For example, the value of  $E$  corresponding to a strain rate of 0.54% per minute is about one-half the value of  $E$  corresponding to a strain rate of 3.33% per minute. The magnitude of Young's modulus found in this manner is considerably smaller than the value found by previous investigators using sonic methods which corresponds to the initial tangent modulus.

This behavior may be illustrated by the Burgers viscoelastic model (Figure 12). Spring  $E_1$  represents the initial tangential modulus. Deformations for strain rates less than infinity will be influenced by the viscous elements  $\eta_1$  and  $\eta_2$ . The slower the strain rate, the lower is the observed Young's modulus. Changes in Young's modulus with the rate of load application are usually attributed to viscous flow. Figure 21 shows the variation of Young's modulus with the strain rate. The average value of Young's modulus plotted nearly linearly with the strain rate. The line drawn through the average values of  $E$  may be represented by the equation

$$E = 19.5 + 9.2 \dot{\epsilon} \dots \dots \dots (10)$$

where  $E$  is the value of Young's modulus and  $\dot{\epsilon}$  is the rate of axial deformation expressed in per cent of height per minute. Any effect of confining pressure upon the value of Young's modulus is obscured by the scatter of results. Since temperature influences the value of Young's modulus (Nakaya, 1959),

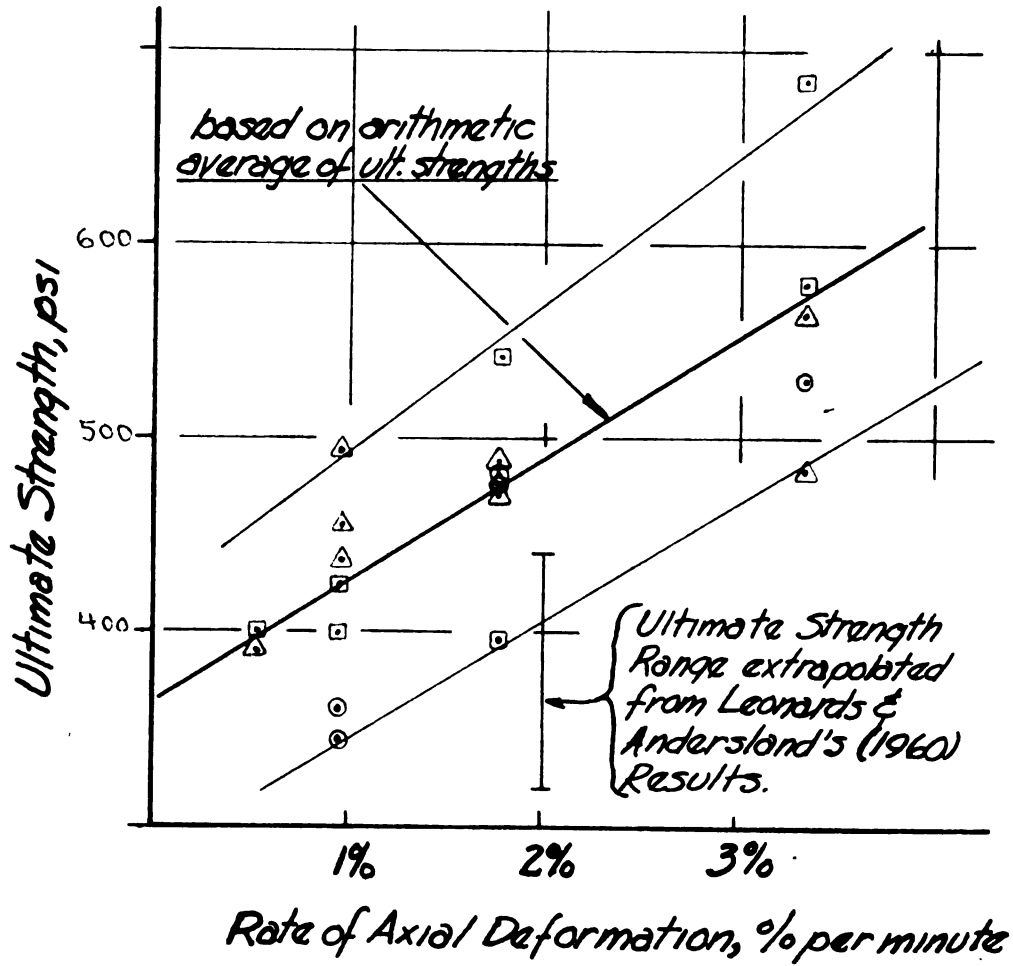


Variation of Young's Modulus of Ice With Strain Rate

Figure 21

the constant in Eq. 10 should increase with decreasing temperature. On the average, tests conducted at lower rates of strain showed less ultimate strength than those strained at higher rates. This behavior is observed in many engineering materials (steel is a good example) where impact tests indicate a larger ultimate strength of the material than those conducted by conventional tension or compression tests. By comparing Figure 20a (strain rate 0.54%) to Figure 21d (strain rate 3.33%), it can be seen that the modes of failure are becoming more brittle.

The arithmetic average of the different ultimate strengths, irregardless of confining pressure, increases linearly with increasing strain rate as shown in Figure 22. The ultimate strengths varied as much as 200 psi. Previous investigators of compressive strength of ice show a similar scatter of results (Butkovich, 1954; Leonards and Andersland, 1960). The magnitudes of compressive strength are in the same range as reported by Butkovich, 1954. Leonards and Andersland (1960) conducted experiments in a manner quite similar to that used in these experiments. They used a constant-rate-of-strain of 2% per minute. The range of ultimate strength obtained by extrapolation of their results is plotted in Figure 22. Their different range may be due to a slightly different technique used in sample preparation. They did not seed the supercooled water, hence less uniform samples may have been obtained.



Temperature  $-4^{\circ}\text{C}$

$\Delta$ , 0 psi;  $\odot$ , 30 psi;  $\square$ , 45 psi; Confining Pressure  $\sigma_3$

Variation of Ultimate Strength of Ice With Strain Rate

Figure 22

An empirical relationship suiting the arithmetic average of the results shown in Figure 22 is

$$\sigma_{ult} = 363 + 63.3 \dot{\epsilon} \dots \dots (11)$$

where  $\sigma_{ult}$  is in psi and  $\dot{\epsilon}$  is the strain rate in per cent of axial deformation per minute. As with the constant in Eq. 10, the constant in Eq. 11 should increase with decreasing temperature.

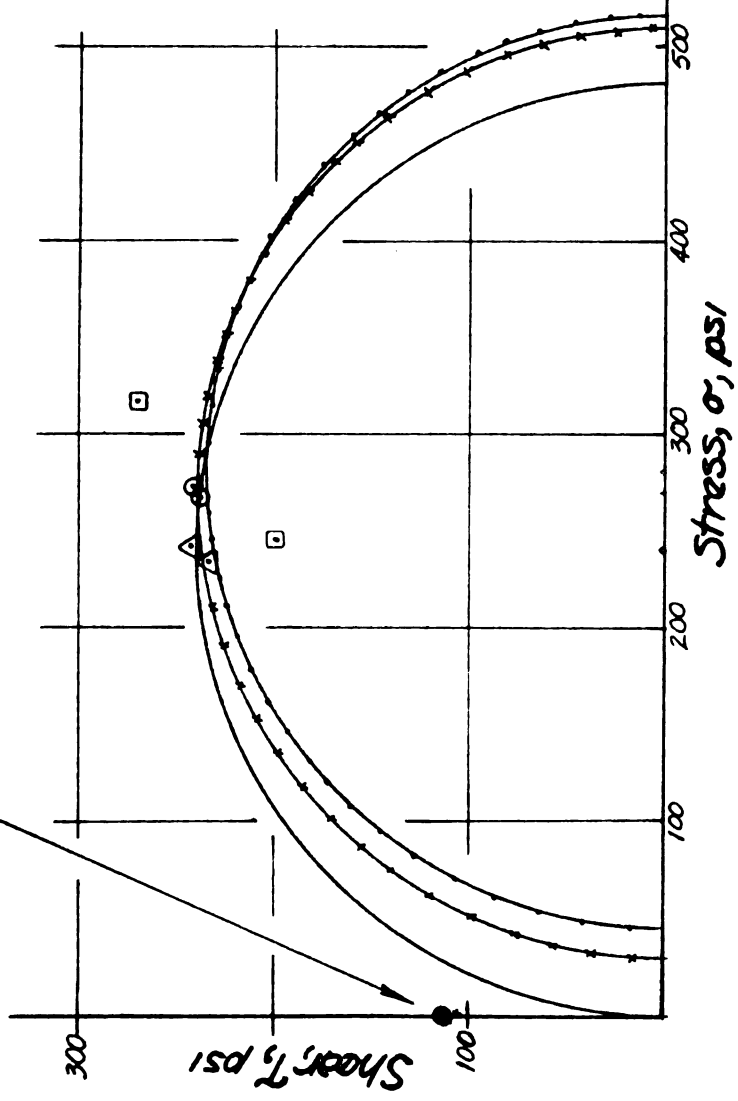
Any relationship between confining pressure and the magnitude of ultimate strength is lost in the scatter of results. In the creep of single ice crystals confining pressure appears to soften the ice crystal. Comparisons between ultimate shear strength and confining pressure are often made using Mohr's circles. If the confining pressure is large enough, ice can no longer exist as a solid. At about 7,160 psi and  $-4^{\circ}$  C, isothermal reversible compression causes the ice to melt, with a subsequent reduction in shear strength to zero. Liquid water is represented by a point on the Mohr diagram. Mohr's failure envelope should slope downward toward this point, indicating a negative angle of internal friction,  $-\phi$ . Mohr's circles drawn for the results of the constant-rate-of-strain experiments neither confirm nor disprove this.

For the range of stresses encountered in frozen soils, the friction angle for ice might well be approximated by zero degrees. Figure 23 shows the Mohr's circles for a strain

Mohr's Circle <sup>1</sup>	Symbol <sup>2</sup>	$\sigma_{3, \text{psi}}$
—	$\Delta$	0
— + —	$\circ$	30
— + — + —	$\square$	45

1. Circles are averages of two specimens.
  2. Actual point of maximum shear stress from individual samples of Note 1.
- Temperature  $-4^{\circ}\text{C}$

Magnitude of Tensile Shear Stress (Lellinek, 1957)  
 $-4.5^{\circ}\text{C}$ ; Rate of Load Application  $> 0.57 \text{ kg/cm}^2 \text{ sec}$ .



Mohr's Circle for Polycrystalline Ice

Figure 23

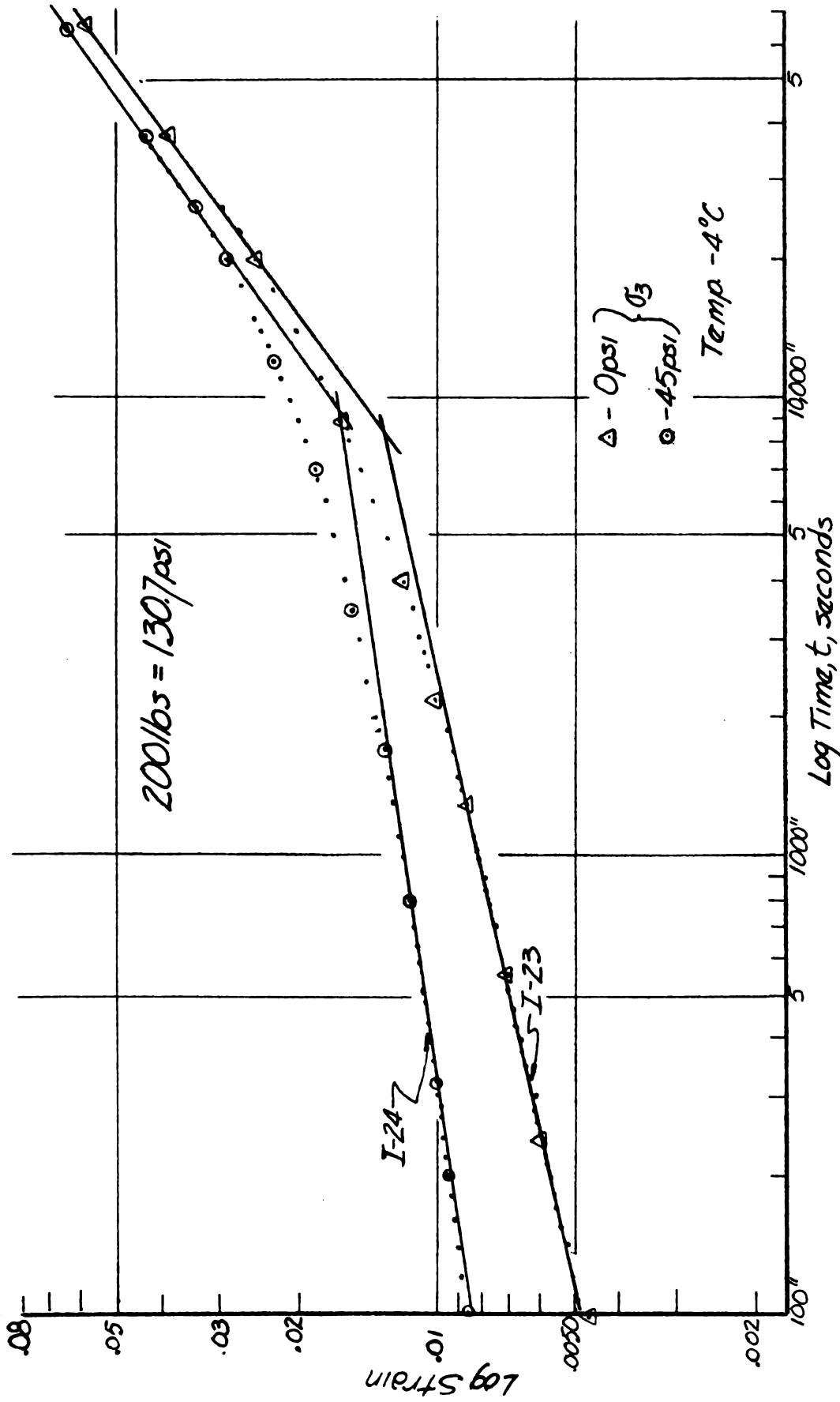
rate of 1.76 per cent per minute. The maximum shearing strength is taken as one-half the diameter of the Mohr's circle of stress. The Mohr's circles plotted represent average results, the actual magnitude of maximum shear strength for individual specimens is shown by symbols. The stress axis is broken to show the liquidus point and the downward slope of the failure envelope.

#### Results of Creep Experiments

Eight polycrystalline ice specimens were used to observe creep properties under constant load. Compressive loads of 200 lbs (130.7 psi), 300 lbs (196.2 psi), and 400 lbs (261.7 psi) were used along with confining pressures of 0 and 45 psi. All results are presented in Figures 24a, b, and c. Good agreement was found between identical samples (Figure 25b) tested under a load of 300 lbs. Although the curves do not fit one upon the other, the rates of creep are in close agreement.

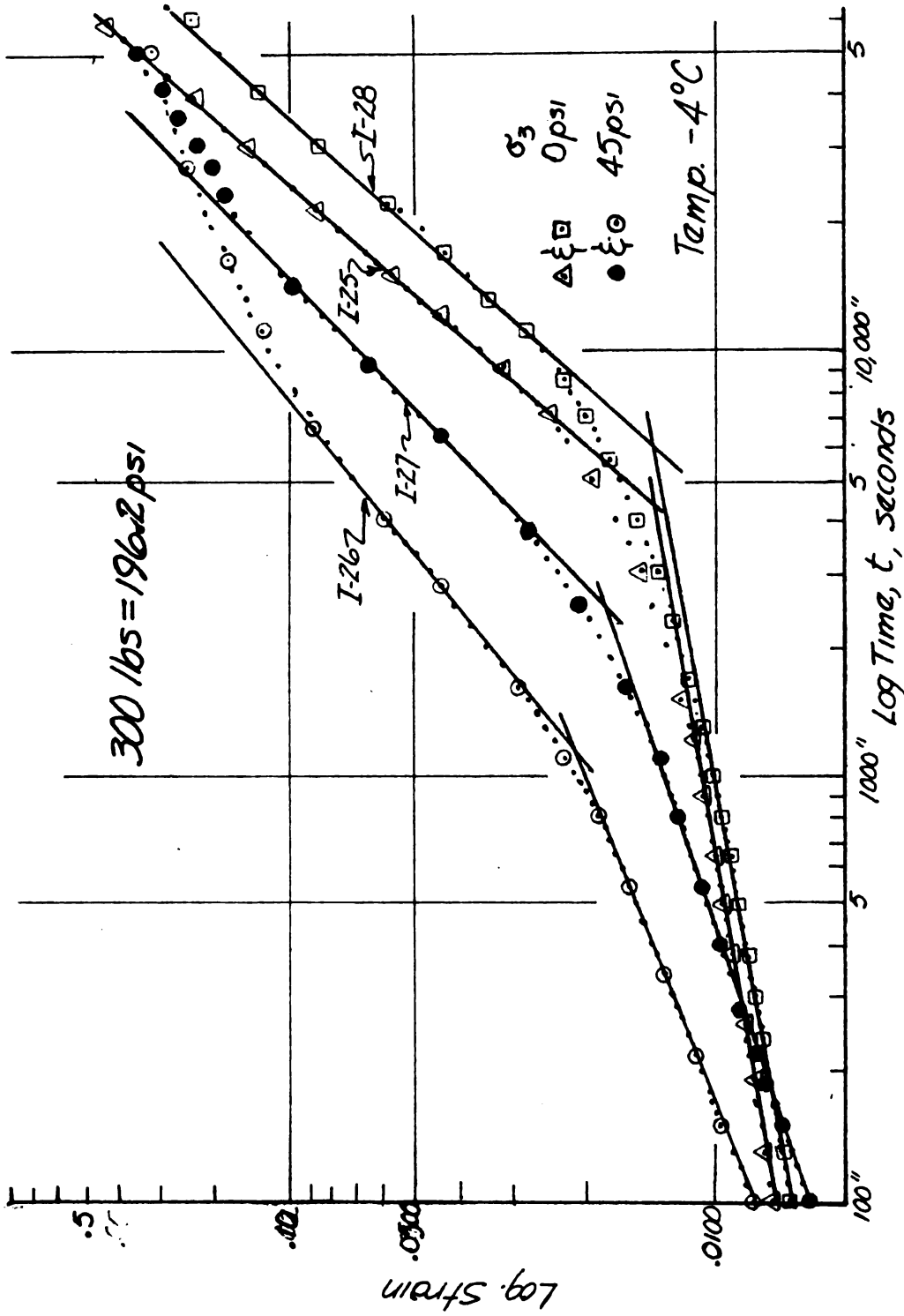
All test loads were approached at a strain rate of 1.76% per minute. Load and deformation readings taken every five seconds made it possible to determine the seating strain for each specimen (values ranged from .0036 to .0081 in/in). The seating strain was subtracted from the strains observed during creep. This technique is similar to that used by Butkovich and Landauer (1959) in which the "elastic" strain was subtracted from following strain readings.

After the tests were completed, inspection showed that



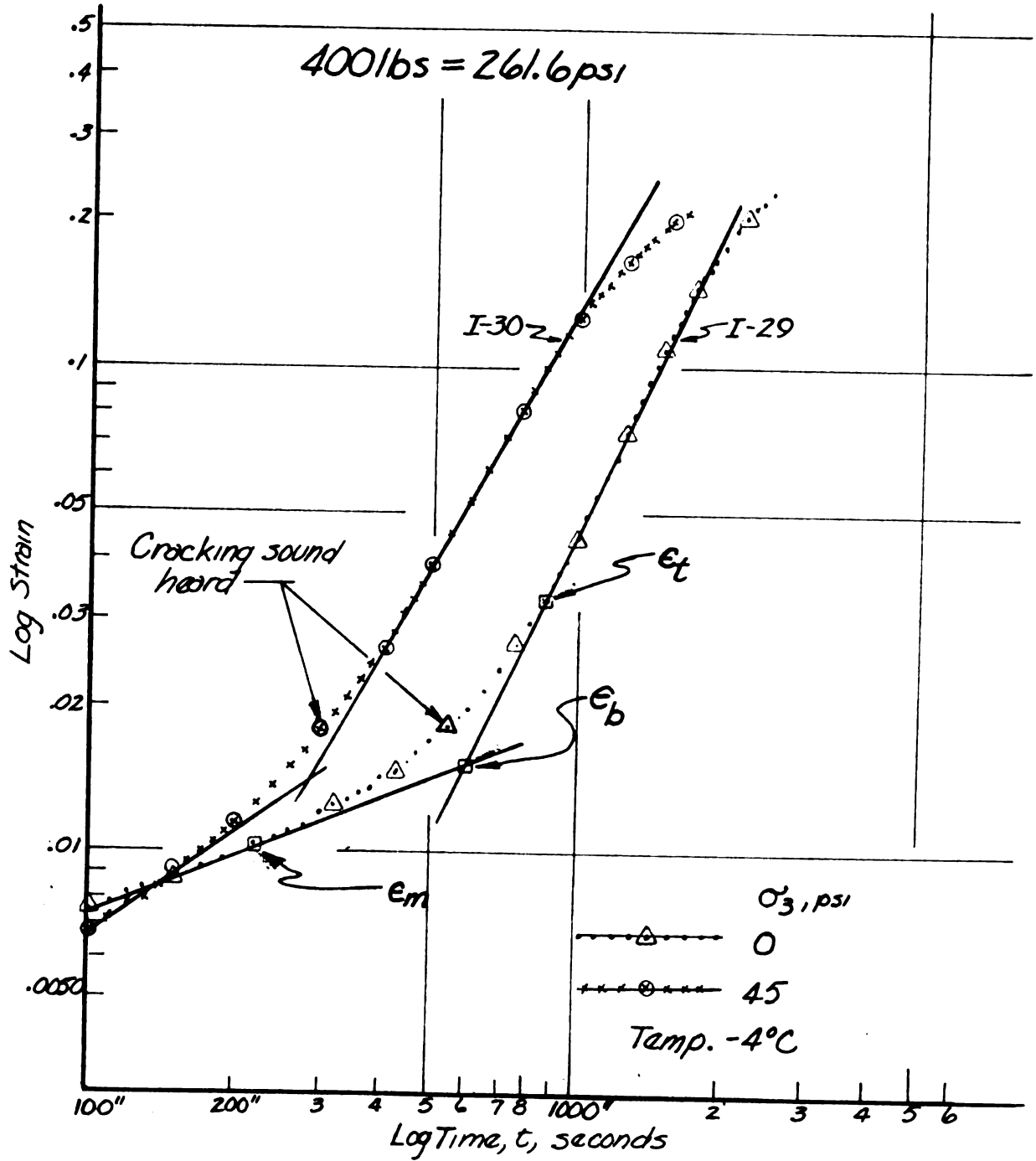
Creep of Ice Under Constant Load, 200 lbs

Figure 24a



Creep of Ice Under Constant Load, 300 lbs

Figure 24 b



Creep of Ice Under Constant Load, 400 lbs

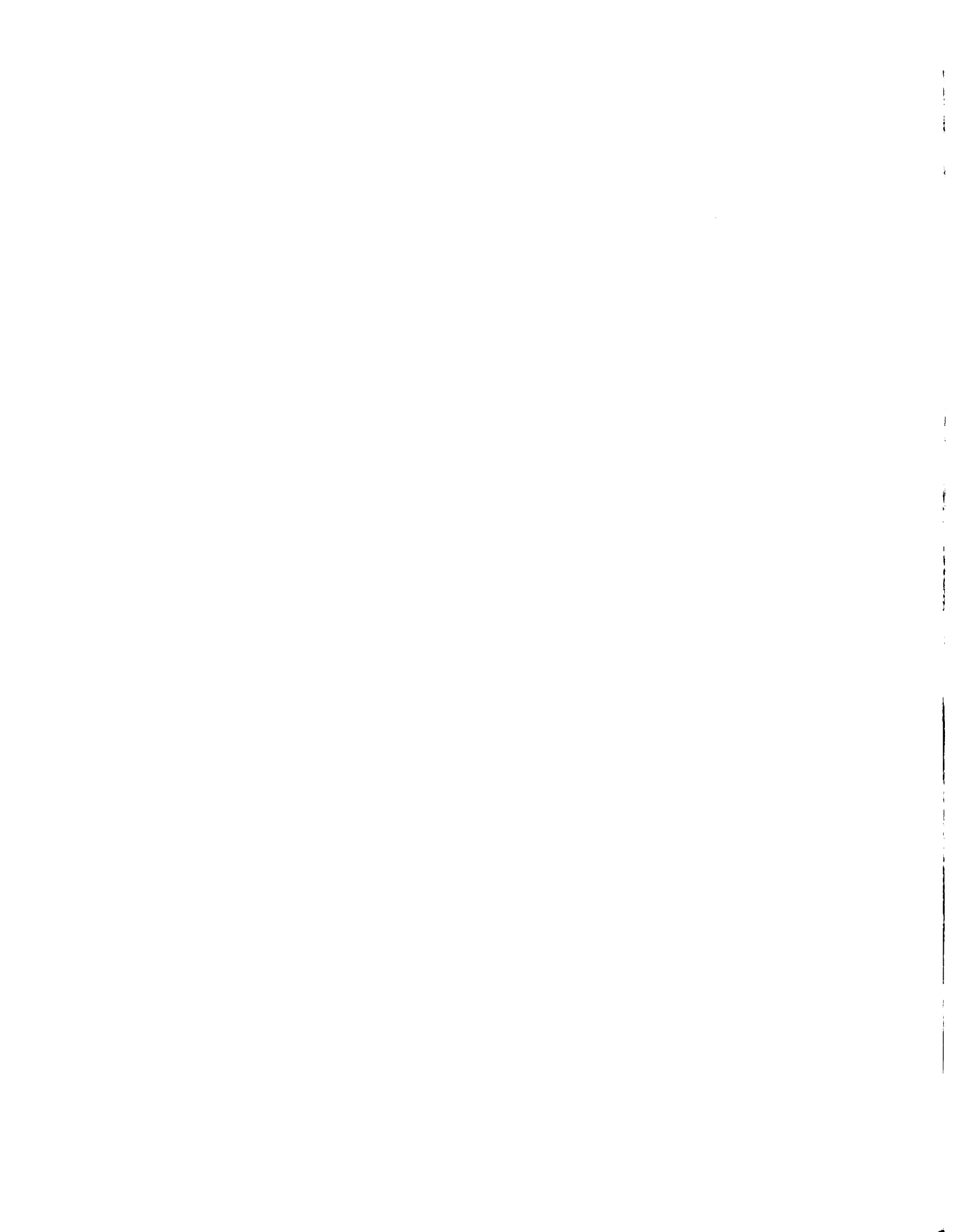
Figure 24c

the majority of creep samples appeared to have failed by bulging. Five of the samples developed "step-like" surfaces (Butkovich and Landauer, 1959), indicating preferential gliding (Figure 18). In addition to bulging, specimens I-29 (400 lbs) and I-30 (400 lbs, 45 psi) appeared to have been shattered internally, similar to the cracked appearance of the constant-rate-of-strain specimens. Cracking sounds were heard during the testing of these specimens (see Figure 24c).

The relationship between time and strain did not prove to be linear (Griggs and Coles, 1954; Jellinek and Brill, 1956; Butkovich and Landauer, 1959; Higashi, 1959). Equations 3a and 3b are unacceptable. However, on a log strain log time plot the creep data becomes linear, showing a minimum creep rate and a tertiary creep rate. Behavioral tendencies observed from the creep curves shown in Figures 24a, b, and c are noted below.

#### Minimum Creep Rate Observations

- 1) The minimum creep rate increased as the stress level increased. Previous investigators of creeping ice have observed this phenomenon. The value of the strain at the beginning of secondary creep was not proportional to the stress level, a necessary condition for a viscoelastic model analysis (Jellinek and Brill, 1956). (See Figure 25a, a summary of Figures 24a, b, and c).
- 2) The minimum creep rate is increased by application



of confining pressure in the majority of experiments. This observation agrees with Rigsby's (1958) observations that confining pressure produces a "softening" of the crystals' bonds. The one exception to this behavior is specimen I-24, creeping under 200 lbs and confined at 45 psi. Since Rigsby's experiments were performed on single ice crystals, no conclusion can be made about the "softening" of polycrystalline ice, as bonding between the individual ice crystals appears to be the controlling factor (Glen and Perutz, 1954; Steinemann, 1954; Glen, 1955, 1958; Butkovich and Landauer, 1959).

Stress level plays a determinant role for the results of the eight creep samples. Values of the exponent  $r$  in equation 1 are computed for the minimum creep rate. It increases with both stress and confining pressure (see Table 4). Equations 1 and 2 are not recommended. (Butkovich and Landauer, 1959).

The technique of variable isolation used by Jellinek and Brill (1956) for equation 4 proved to be difficult to use. For the 400 lb creep curves, values of strain at 1,000 and 2,000 seconds had to be extrapolated in order to plot the stress-strain at constant time (see Figure 25b). Analysis of creep specimens by this technique was not successful. The value of  $n$  varied between 0.60 and 1.13. At only one time

TABLE 4  
SUMMARY OF CREEP RESULTS

Sample	Load	$\sigma_1$ psi	$\sigma_3$ psi	$\epsilon_m$	$\epsilon_b$	$\epsilon_t$	$t_{min}$	$t_{tert}$
I-23	200	130.7	0	.0095	.0129	.0265	.223	.721
I-25	300	196.2	0	.0109	.0140	.0265	.176	1.145
I-28	300	196.2	0	.0105	.0140	.0258	.179	1.125
I-29	400	261.7	0	.0109	.0150	.0290	.398	2.086
I-24	200	130.7	45	.0129	.0162	.0273	.143	.677
I-26	300	196.2	45	.0175	.0212	.0265	.397	.802
I-27	300	196.2	45	.0145	.0182	.0278	.335	.952
I-30	400	261.7	45	.0098	.0140	.0260	.704	1.711

$\epsilon_m$ , strain at end of minimum creep rate

$\epsilon_b$ , strain at assumed beginning of tertiary creep

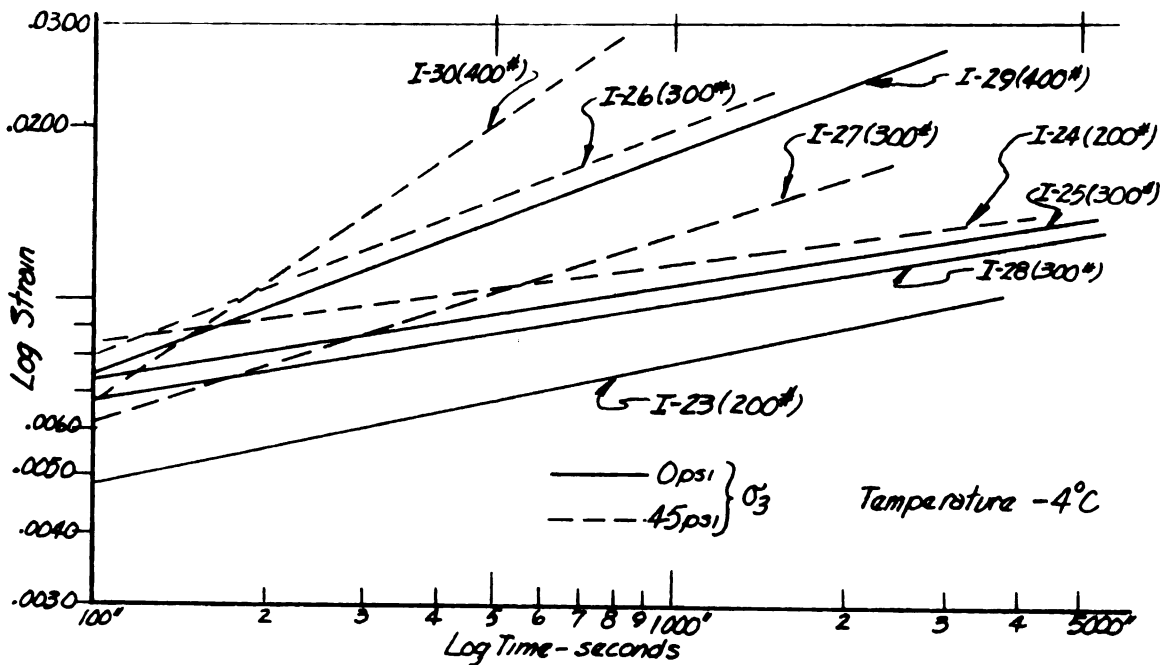
$\epsilon_t$ , strain where tertiary creep is completely established

$t_{min}$ , exponent of Eq. 1 for minimum creep

$t_{tert}$ , exponent of Eq. 1 for tertiary creep.

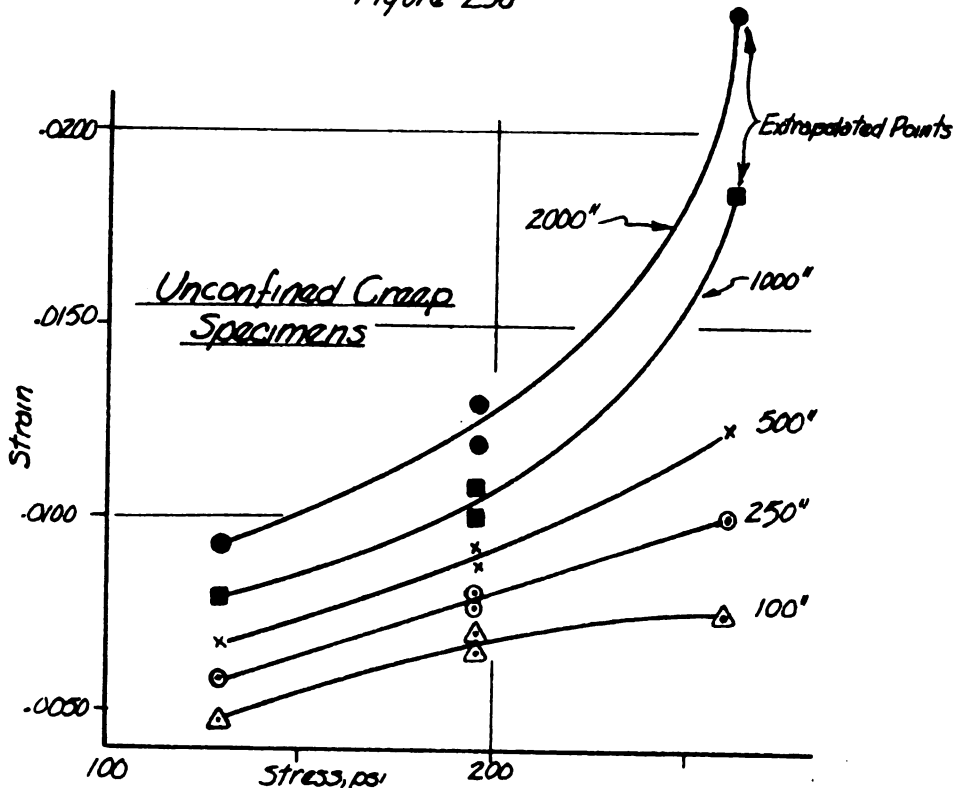
level,  $t = 250''$ , did a linear relationship exist when Figure 25b was replotted as log stress versus log strain. The corresponding value of  $n$  for  $t = 250''$  was 0.80.

Specimens I-29 and I-30 were taken from the last batch of identical specimens having a slightly lower density than



Variation of Minimum Creep Rate With Load and Confining Pressure

Figure 25a



Stress-Strain Curves of Constant Time Intervals, Secondary Creep Stage

Figure 25b

Variation of Minimum Creep With Load, Time, and Confinement  
Figure 25

the other batches. These specimens should and did exhibit faster creep rates. If the creep rates of these samples were somewhat lower, the value of  $n$  within the limits given in the preceding paragraph would satisfy Eq. 4.

Using  $n = 0.80$ , the exponent of the time variable  $m$  was determined using the previously discussed technique. Jellinek and Brill (1956) show the relationship with all their results plotting on one line. The creep results showed different slopes for each sample.<sup>1</sup> Three samples had comparable results for which  $m$  was approximately 0.20. These three samples, I-23, (200 lbs), I-27 (300 lbs) and I-28 (300 lbs) were not subjected to confining pressure. The specimens subjected to confining pressure had larger exponents for both  $m$  and  $n$  (except sample I-24; 200 lbs, 45 psi). No basic relationship could be found between the respective magnitudes of the exponents for confined specimens and the magnitudes of the unconfined specimens.

The minimum creep rate of ice under high stress and confinement was non-linear to such a degree that representation of behavior by a viscoelastic model is untenable. Higashi (1959) reached a similar conclusion in his study of ice under hydrostatic pressure.

Griggs and Coles (1954) also observed the nonlinearity of time and strain in creep specimens. Their empirical

---

<sup>1</sup>A similar plot using tertiary creep is shown in Figure 27, using  $n = 1.0$ .

relationship for single ice crystals, Eq. 5, includes the temperature parameter. Rigsby's (1958) findings suggest that confining pressure is also a parameter. Using Eq. 4 as a framework, both temperature and confining pressure can be included in an empirical relationship compatible with observed behavior, generally

$$\epsilon = a \left[ \sigma_1 + f(\sigma_3) - f(T_0) \right]^n t^m \dots (12)$$

where  $f(\sigma_3)$  and  $f(T_0)$  mean function of confining pressure and temperature below freezing, respectively.

The minimum creep rate data was programmed on the Michigan State University digital computer, MISTIC, for equation 12. Values of  $m$  and  $n$  were allowed to vary from .6 to 2.0 and from .6 to 4.5, respectively. Various functions of  $\sigma_3$  were tried, as follows:

$$\mu \sigma_3, \sqrt{\sigma_3}, + \sigma_3 \text{ and } -\sigma_3^{\cdot 1}$$

0.3 was used for the value of  $\mu$ , Poisson's ratio (Jellinek and Brill, 1956). The computer was asked to solve for the constant  $a$ . Trends observed from the variability of the constant value,  $a$ , indicate:

- 1)  $m$  will be less than 0.6, probably between 0.2 and 0.35.
- 2)  $n$  will probably be less than one. The value at 0.8 worked well.

---

The effect of using  $-\sigma_3$  as a function can be seen in Figure 25, lines A and A<sup>1</sup>.

- 3) The function of  $\sigma_3$  which produced the best results was  $+\sigma_3$ . Higher powers of  $\sigma_3$  may produce better answers.

For the prediction of creep, an empirical relationship in the form of Eq. 12 appears to be the most suitable.

#### Tertiary Creep Observations

- 1) The time taken to begin tertiary creep decreased as the load level was increased.
- 2) Tertiary creep rate increases with the load. Triaxial test results agree with results using other methods. (Steinmann, 1954).
- 3) Tertiary creep rate was decreased by confining the sample.

Values for the exponent  $r$  in Eq. 1 were computed to show the influence of confinement and load level. They are listed in Table 4.

The behavior of the tertiary creep rate can be observed in Figure 26. Once again difficulties arose when using the analysis technique presented by Jellinek and Brill (1956). Values of  $n$  in Eq. 4 for tertiary creep could not be obtained in this manner because time could not be isolated.

By assuming a value of  $n = 1$ , the exponent of the time variable,  $m$ , was computed from the slopes of the lines in Figure 27. The straight lines representing the tertiary creep rate became apparent when they were compared to a fixed point extrapolated from each specimen's creep curve.



The fixed point was the "beginning" of tertiary creep.

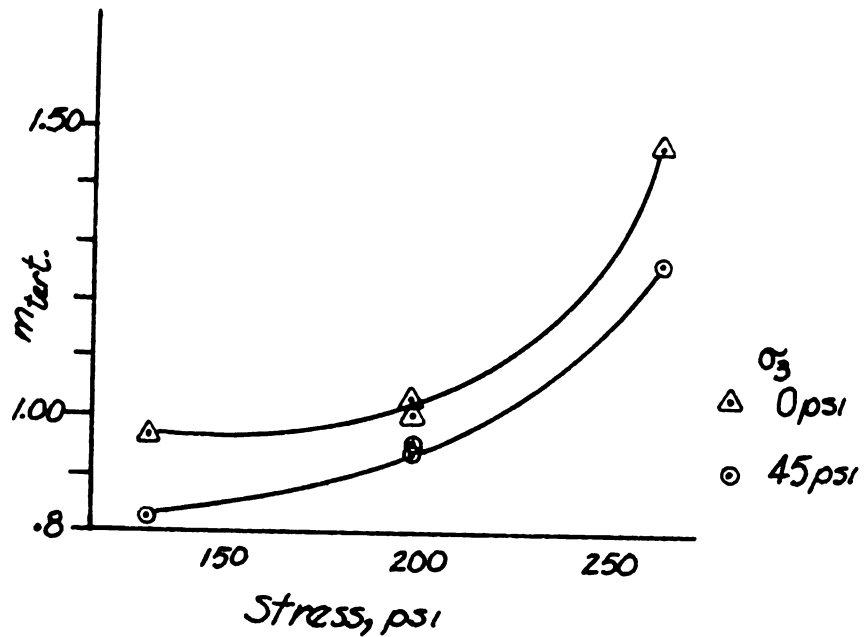
The beginning of tertiary creep is assumed as the intersection of the minimum creep line with the tertiary creep line, symbolized by  $\epsilon_b$ .  $\epsilon_b$  agreed well from test to test, varying in values of strain from 1.4% to 2.1%, averaging at 1.5%. The strain at the end of the minimum creep stage, i.e., the point at which the creep curves start a transition into tertiary creep, is designated as  $\epsilon_m$ . The point at the end of the transition into tertiary creep is designated as  $\epsilon_t$  (see Figure 25c). Values of strain at these points are listed in Table 4.

Values of  $m$  varied with the stress level as is shown in Figure 27. The interesting observation is that the effect of confinement is very nearly constant. The relationship between  $m$  unconfined and  $m$  confined at 45 psi is as follows:

$$m_{45 \text{ psi}} = \frac{m_{\text{unconf}}}{1.13} \dots \dots \dots (13)$$

The nonlinearity of  $m$  with stress level made the use of a viscoelastic model to represent tertiary creep unsatisfactory.

Several observations can be made by comparing the results of the constant rate of strain experiments to the creep experiments as shown in Figure 28. For the constant-rate-of-strain experiments, values of strain at the beginning of the plastic response (end of the elastic response) and the strain at ultimate load are listed in Table 3. They are denoted by  $\epsilon_p$  and  $\epsilon_{\text{ult}}$  respectively. The listed



$$m_{45\text{psi}} \approx m_{\text{unconf.}} \\ 1.13$$

Variation of the Exponent of Time for Tertiary Creep  
With Load and Confinement

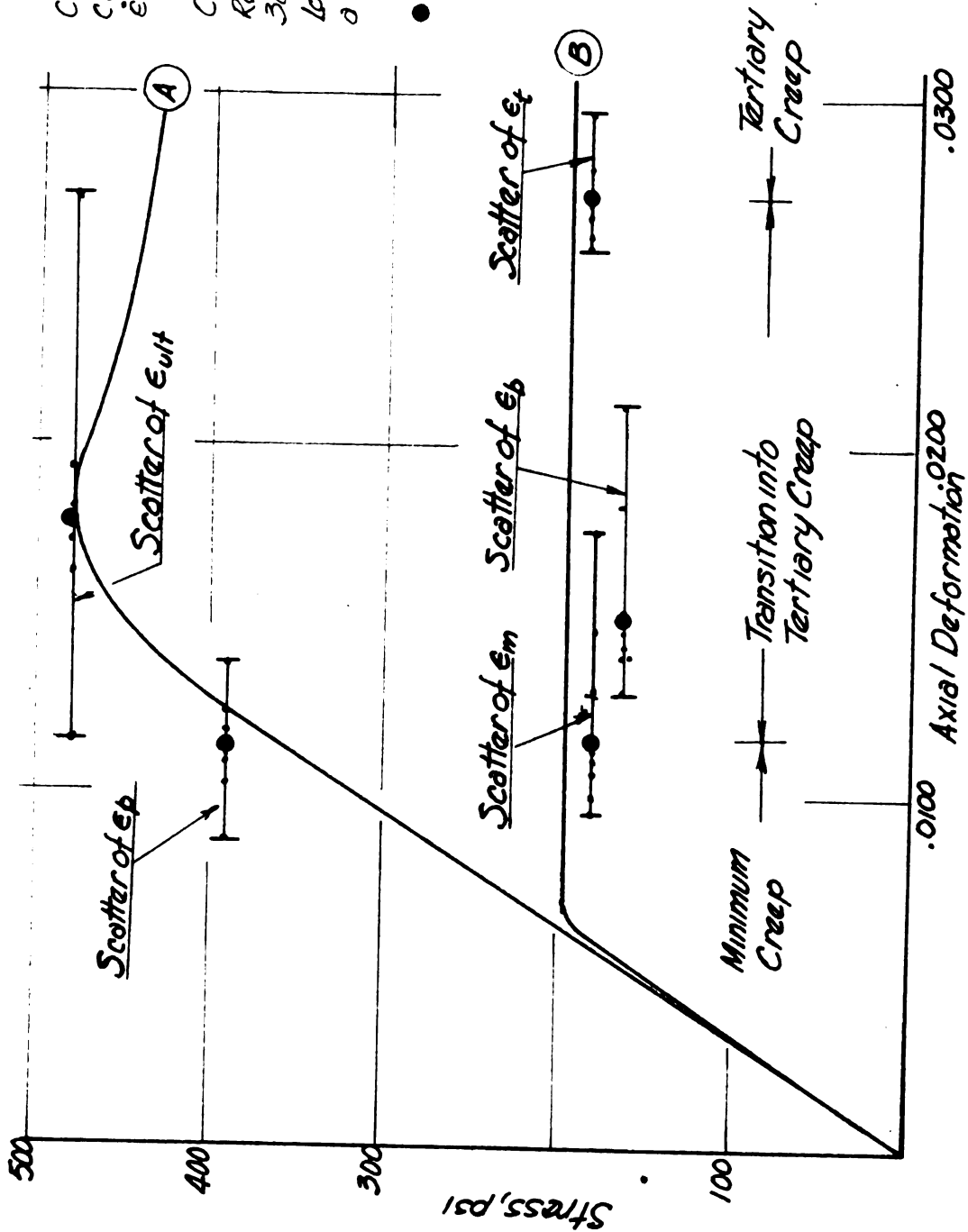
Figure 27

values have been corrected for seating strain, and were obtained by interpolation of the stress-strain curves, Figures 20a, b, c, and d.

The arithmetic average strain value for the beginning of the plastic zone,  $\epsilon_p$ , was 0.0108. The strain value for ten of the specimens was within  $\pm .0008$  of this value. Sixteen of the samples were within  $\pm .0018$  of the average value. It appears, then, that in the neighborhood of 0.0108 strain, the polycrystalline ice samples begin another behavioral trend. This behavior was also noticed in the creep specimens where the average strain value at the end of the secondary creep stage,  $\epsilon_m$ , was 0.0113 (see Figure 28). Creep strains were also computed by subtracting the extrapolated seating strain. It appears that  $\epsilon_p$  is approximately equal to  $\epsilon_m$ .

This raises the question, how is tertiary creep related to the ultimate strength of ice? A comparison of these two phenomena might be made by considering the relative amounts of energy supplied to a specimen that would produce these behavioral characteristics. Energy calculations would necessarily be based upon the theory of plasticity (Hill, 1956), and they would involve measurements beyond the capabilities of the apparatus and technique used.

This question can be answered, in part, by a comparison of the strains occurring at the beginning of tertiary



Curve A is the Stress-Strain Curve for Specimen I-12,  $\dot{\epsilon} = 1.76\%$  per minute.

Curve B is the stress-strain Representation of a Typical 300 lb. Creep Curve. Creep loads were Reached by applying a  $\dot{\epsilon}$  of 1.76% per minute.

- Represents the average of the Scattered Stress. The small dots are individual strain values, no attempt is made to correlate stress to strain.

Comparison of a Typical Stress-Strain Curve To a Typical Creep Curve

Figure 28

creep,  $\epsilon_p$ , the ultimate strain,  $\epsilon_{ult}$ , and the strain at which tertiary creep has been completely established,  $\epsilon_t$ . This comparison may be made from strain values listed in Tables 3 and 4. The scatter of results is shown graphically in Figure 28 which shows the observed behavior of a specimen tested at a strain rate of 1.76%, i.e. the same strain rate at which the creep samples were subjected to during application of their respective loads.

The average strain at which tertiary creep is established,  $\epsilon_t$ , was observed to be larger than the average ultimate strain,  $\epsilon_{ult}$ .  $\epsilon_p$  was found to be slightly less than  $\epsilon_{ult}$ , but considering the scatter of results, their values are comparable to each other. All observations concerning characteristic strains of polycrystalline ice can be stated approximately by

$$\epsilon_p \cong \epsilon_m < \epsilon_{ult} < \epsilon_t \dots \dots \dots (14)$$

The magnitude of strain at the beginning of plasticity is approximately equal to the strain at the end of minimum creep. These strain values are less than strain at the "beginning" of tertiary creep, and the ultimate strain, whose magnitudes are comparable. The magnitude of ultimate strain is less than the strain at which tertiary creep has been completely established.

Previous investigators have hinted that tertiary creep

begins after the bonds have been broken between the individual crystals of polycrystalline ice. It seems logical to assume that tertiary creep begins when the ultimate strength of the material has been surpassed. This hypothesis cannot be entirely supported by the results, but based on the observed strains it appears to be verified.

Observations made during the creep of the specimens under a 400 lb load imply that the ultimate strength of these two specimens had been reached during the transition into tertiary creep. A slight cracking sound was heard similar to that which was sometimes heard as a constant-rate-of-strain specimens reached their ultimate strength. In order to keep the load at 400 pounds, additional hydraulic pressure had to be applied to the loading head of the testing machine through its needle valve.

The hypothesis is further supported by observations made on confined tertiary creep. Assuming the bonds between the individual crystals had been broken, gliding would proceed almost entirely by movements between the crystals. The tertiary creep rate would represent a resistance created by friction between their surfaces. The effect of confining pressure would create additional friction, retarding the movement of the crystals, which in turn would be observed through a lower tertiary creep rate. This effect of confinement can be observed from Eq. 13. In addition, the reduction in tertiary creep by a confining pressure of 45 psi was very

nearly a constant, indicating that a comparable amount of resistance to flow was created, irregardless of the load used for creep. This behavior supports the concept that the intercrystalline bonds have been disrupted.

The nonlinearity of observed strains with stress in both secondary and tertiary creep support Higashi's (1959) conclusions concerning the exponent  $n$  in equation 4.  $n$ 's value increases as the creep load increases. The previous implication that the activation energy of ice may be dependent upon stress level is also supported by this non-linearity.

## CHAPTER V

### CONCLUSIONS

From the observed results of the experiments conducted on duplicate samples of polycrystalline ice at  $-4^{\circ}\text{C}$  and for the techniques used in this study the following general observations are made.

- 1) Duplication of tests is a necessity, as even carefully duplicated polycrystalline samples produced a large scatter of results.
- 2) The value of Young's modulus in compression is highly dependent upon the rate of strain application. An approximate relationship between Young's modulus and the strain rate would be:

$$E = 19.5 + 9.2 \dot{\epsilon} \quad ; \quad 0.5\% < \dot{\epsilon} < 3.33\%$$

where  $E$  is in kips per square inch and the strain rate,  $\dot{\epsilon}$ , is expressed in per cent of height per minute.

- 3) The ultimate strength of ice increases with increased rate of strain application. An approximate relationship between ultimate strength and strain rate would be

$$\sigma_{\text{ult}} = 363 + 63.3 \dot{\epsilon} \quad ; \quad 0.5\% < \dot{\epsilon} < 3.33\%$$

where the ultimate strength is in pounds per square inch and the strain rate is as previously defined.

- 4) The use of a viscoelastic model or simple bulk flow formula to represent creep of ice under high stress appears to be untenable except for approximate relationships.
- 5) The effect of confining pressure upon the creep of ice under high stress appears to increase the minimum creep rate and to decrease the tertiary creep rate. Further studies are needed to determine the actual influence of confining pressure.
- 6) The total strain values at the end of the elastic response for the constant-rate-of-strain experiments agrees well with the total strain at the end of the minimum creep state for the creep results.
- 7) Using a similar comparison of strain values, the ultimate strain at failure in the constant-rate-of-strain experiments compares with the assumed "beginning" of the tertiary creep curve.
- 8) Based on strain measurements and supported by conclusion number five, it is likely that constant tertiary creep begins after the ultimate strain of the polycrystalline samples has been exceeded.

## RECOMMENDATIONS FOR FURTHER RESEARCH

Further research is needed in several areas related to the mechanical properties of ice. Specific problems are briefly described below:

1. Study the effect of large confining pressures at constant temperatures to determine the shape of Mohr's rupture envelope. The angle of internal friction for ice should be investigated when the difference between the melting point and test temperature is held constant similar to the technique used by Rigsby (1958).

2. Study the relationship between activation energy and more conventional bulk flow laws. There is an indication that  $H$  is dependent upon stress.

3. Study the relationship between the creep curves of a frozen fine grained soil and polycrystalline ice. A further comparison with duplicate unfrozen soil specimens may provide answers to some of the more fundamental questions about frozen soil mechanics.

4. Determine the Universal Stress-Strain Curve for ice (Hill, 1956) in order that comparisons can be made between constant-rate-of-strain experiments and constant-rate-of-stress-application experiments. Once it is determined, the tensile strength of ice (Jellinek, 1957) might be compared to the compressive strength of ice.

## BIBLIOGRAPHY

- Bjerrus, Niels. "Structure and Properties of Ice." Science Vol. 115, London, England, 1952, pp. 385-390.
- Butkovich, T.R. Ultimate Strength of Ice. U.S. Army Snow, Ice, and Permafrost Research Establishment, Corps of Engineers, hereinafter referred to as SIPRE, Research Paper 11, Wilmette, Illinois, December, 1954.
- \_\_\_\_\_, and J.K. Landauer. The Flow Law for Ice. SIPRE Research Report 56, August, 1959.
- Chalmers, Bruce. The Growth of Ice in Supercooled Water. (Edgar Marburg Lecture, 64th Annual Meeting of the Amer. Soc. for Testing and Materials, October, 1961, Philadelphia, Pa.)
- Finnie, I. and W.R. Heller. Creep of Engineering Materials. New York, New York: McGraw-Hill Book Co., Inc., 1959.
- Glen, J.W. "The Creep of Polycrystalline Ice." Proceedings of the Royal Society of London, Vol. 228, 1175, Series A, London, England: Royal Society, March, 1955, pp. 519-538.
- \_\_\_\_\_. "The Mechanical Properties of Ice." Advances in Physics, Vol. 7, London, England: Taylor and Francis Ltd., 1958, pp. 254-258.
- \_\_\_\_\_, and M.F. Perutz. "The Growth and Deformation of Ice Crystals." Journal of Glaciology, Vol. 2, Cambridge, England: British Glaciological Society, 1954, pp. 397 to 403.
- Goldman, J.E. "Structure and Viscoelastic Properties of Amorphous." The Science of Engineering Materials, New York, New York: John Wiley & Sons, Inc., 1957, pp. 472-479.
- Griggs, D.T. and N.E. Coles. Creep of Single Crystals of Ice. SIPRE Report 11, 1954.
- Halvorsen, L.K. Determination of the Modulus of Elasticity of Artificial Snow-Ice in Flexure. SIPRE Research Report 31, February, 1959.

- Higashi, A. Plastic Deformation of Hollow Ice Cylinders Under Hydrostatic Pressure. SIPRE Research Report 51, July, 1959.
- Hill, R. The Mathematical Theory of Plasticity. Oxford, England: Oxford at the Clarendon Press, 1956.
- Jackson, K.A. and B. Chalmers. Study of Ice Formation in Soils. (Arctic Construction and Frost Effects Laboratory, for Office of the Chief of Engineers, Airfields Branch, Engineering Division, Military Construction, Technical Report No. 65, November, 1957.) Boston, Massachusetts: U.S. Army Corps of Engineers, 1957.
- Jastrzebski, Z.D. Nature and Properties of Engineering Materials. New York, New York: John Wiley & Sons, Inc., 1959.
- Jellinek, H.H.G. Tensile Strength Properties of Ice Adhering to Stainless Steel. SIPRE Research Report 23, January, 1957.
- \_\_\_\_\_, and R. Brill. "Viscoelastic Properties of Ice." Journal of Applied Physics, Bul. 27; 10, New York, New York: Amer. Inst. of Physics, October, 1956.
- Kamb, W.B. "The Glide Direction in Ice." Journal of Glaciology, Vol. 3, Cambridge, England: British Glaciological Society, October, 1961, 1097-1106.
- Landauer, J.K. Creep of Snow Under Combined Stress. SIPRE Research Report 41, December, 1957.
- \_\_\_\_\_. Growing of Large Single Crystals of Ice. SIPRE Report 48, July, 1958.
- Leonards, G.A. and O.B. Andersland. "The Clay Water System and Shearing Resistance of Clays." Research Conference on the Shearing Strength of Cohesive Soils, Soil Mechanics and Foundations Division, Amer. Soc. of Civil Engineers, University of Colorado, Boulder, Colo., June, 1960, pp. 793-817.
- Lovell, C.W., Jr. Temperature Effects on Phase Composition and Strength of Partially-Frozen Soil. Highway Research Board Bulletin 168, Washington, D.C., 1957.
- Martin, R. Torrence. "Rhythmic Ice Banding in Soil?" Frost Effects in Soils and on Pavement Surfaces, Highway Research Board Bulletin 218, Washington, D.C., 1959.
- Nakaya, U. Mechanical Properties of Single Crystals of Ice. SIPRE Research Report 28, October, 1958.

- . Viscoelastic Properties of Snow and Ice in the Greenland Ice Cap. SIPRE Research Report 46, May, 1959.
- Richards, E.W. Engineering Materials Science. San Francisco, California: Wadsworth Publishing Co., Inc., 1961.
- Rigsby, G.P. "Effect of Hydrostatic Pressure on Shear Deformation of Single Ice Crystals." Journal of Glaciology, Vol. 3, Cambridge, England: British Glaciological Soc., October, 1958, pp. 273-278. (Originally published as SIPRE Research Report 32.)
- Scott, R.B. "The Calibration of Thermocouples at Low Temperatures." Temperature, Its Measurement and Control in Science and Industry, (Amer. Inst. of Physics and National Bureau of Standards, National Research Council) New York, New York: Reinhold Publishing Corp., 1941, pp. 206-218.
- Secor, K.E. and C.L. Monismith. "Analysis of Triaxial Test Data on Asphalt Concrete Using Viscoelastic Principles." Proceedings of the Highway Research Board, Vol. 40, The Highway Research Board, Washington, D.C., January, 1961, pp. 295-314.
- Serata, S. (Asst. Professor of Sanitary Engineering, Michigan State University), Personal communication, December, 1961.
- Skempton, A.W. "Effective Stress in Soils, Concrete and Rocks." Pore Pressure and Suction in Soils. London, England: Bulterworths, Inc., 1961.
- Steinemann, Samuel. "Results of Preliminary Experiments on the Plasticity of Ice Crystals." Journal of Glaciology, Vol. 2, Cambridge, England: British Glaciological Soc., 1954, pp. 404-412.
- Stephens, R.W.B. "The Mechanical Properties of Ice. The Elastic Constants and Mechanical Relaxation of Single Crystal Ice." Advances in Physics, Vol. 7, London, England: Taylor and Francis Ltd., 1958, pp. 266-275.
- United States Army Corps of Engineers, The Frost Effects Laboratory. Investigation of Description, Classification, and Strength Properties of Frozen Soils. SIPRE Report 8 Fiscal Year 1951, June, 1952.
- Van Vlack, L.H. Elements of Materials Science. Reading, Mass.: Addison-Wesley Publishing Co., Inc., 1959.

**APPENDIX A**

**Detailed Procedures**

### Mounting A Frozen Sample In The Triaxial Cell

A Leonards-Farnell Triaxial Cell was used as a test cell. The top and cylindrical sides are built as one piece; the base is separate.

To place a sample in the cell, a technique was developed which exposed the frozen sample to a minimum of warming. Samples were carried from cold storage ( $-15^{\circ}$  C) to the test cell in a pre-chilled brass membrane stretcher and immediately mounted in the test cell. The test cell was submerged in the coolant bath, which was colder than the test temperature. The sample mount on the test cell base was not entirely submerged. The sample was placed on this projection and the surplus of its two membranes rolled over the mount. A heavy natural rubber membrane was then placed over the sample and mount, and the thermocouple inserted between this new membrane and the sample.

The test cell was then taken from the bath and placed in its proper position on the cell base. The piston was lowered and seated on the piston cap, after which the top of the cell was secured to the base plate. The piston was then locked in place so that the sample would not become unseated during moving.

The test cell was allowed to fill while submerged in the coolant bath. It was then placed in the filled and circulating test tank. Pressure was applied to the system

either by opening the cell stopcock, (0 psi), or applying pressure by means of the hydraulic system, (30 psi and 45 psi).

#### Calculation of Stress

In the constant rate of strain experiments, the observed deformations were converted into unit axial strain. As the sample was compressed, the average cross-sectional area became larger. Based on the theory of plasticity, (Hill, 1956), this enlargement was accounted for in the calculation of stress by:

$$\sigma = \frac{P}{A_1}$$

when the corrected area,  $A_1$ , is given by

$$A_1 = A_0 \sqrt{\epsilon\text{-strain}}$$

$A$  is the cross-sectional area at the beginning of the experiment. In the creep experiments no adjustment was made to account for the increasing cross-sectional area. This increase in area was small, hence the creep curves produced are assumed to be a constant load.

**APPENDIX B**

**Data**

TABLE 5  
SEATING STRAIN OBSERVATIONS

Sample	Seating Strain in/in	Stress at Beginning of Elastic Response, psi
I-1	.0105	73
I-2	.0079	105
I-4	.0018	76
I-5	.0037	96
I-6	.0035	92
I-7	.0037	115
I-8	.0033	109
I-9	.0050	80
I-10	.0050	90
I-11	.0064	106
I-12	.0063	72
I-13	.0081	68
I-14	.0071	70
I-15	.0070	72
I-16	.0068	118
I-17	.0104	195
I-18	.0073	129
I-19	.0101	163
I-20	.0096	180
I-21	.0069	230
I-23	.0038	73
I-24	.0036	67
I-25	.0037	48
I-26	.0068	71
I-27	.0054	70
I-28	.0054	67
I-29	.0081	80
I-30	.0037	70

ROOM USE ONLY

MAR 16 1966

101

~~1872~~ 101

MICHIGAN STATE UNIV. LIBRARIES



31293000096788